

Rotating matter waves in Bose–Einstein condensates

Todd Kapitula^a, P.G. Kevrekidis^b, R. Carretero-González^{c,*}

^a *Department of Mathematics and Statistics, University of New Mexico, Albuquerque, NM 87131, United States*

^b *Department of Mathematics and Statistics, University of Massachusetts, Amherst, MA 01003-4515, United States*

^c *Nonlinear Dynamical Systems Group¹, Department of Mathematics and Statistics, San Diego State University, San Diego, CA 92182-7720, United States*

Received 26 September 2006; received in revised form 25 May 2007; accepted 19 June 2007

Available online 27 June 2007

Communicated by J. Lega

Abstract

In this paper we consider analytically and numerically the dynamics of waves in two-dimensional, magnetically trapped Bose–Einstein condensates in the weak interaction limit. In particular, we consider the existence and stability of azimuthally modulated structures such as rings, multi-poles, soliton necklaces, and vortex necklaces. We show how such structures can be constructed from the linear limit through Lyapunov–Schmidt techniques and continued to the weakly nonlinear regime. Subsequently, we examine their stability, and find that among the above solutions the only one which is always stable is the vortex necklace. The analysis is given for both attractive and repulsive interactions among the condensate atoms. Finally, the analysis is corroborated by numerical bifurcation results, as well as by numerical evolution results that showcase the manifestation of the relevant instabilities.

© 2007 Elsevier B.V. All rights reserved.

Keywords: Bose–Einstein condensates; Nonlinear Schrödinger equation; Lyapunov–Schmidt; Vortices

1. Introduction

In the past few years, the dynamics of Bose–Einstein condensates (BECs) have become a topic of intense theoretical and experimental investigation as has been evinced by numerous recent books [47,48] and review articles [16,32,34,37,39,44]. This development has accentuated the interest of the nonlinear wave community in nonlinear Schrödinger type equations. This is because at the mean-field level [16,47,48] the inter-atomic interactions in the BECs can be approximated very well by a pair interaction potential in the form of a δ -function, which, in turn, leads to a quartic term in the mean-field Hamiltonian and therefore to a nonlinear Schrödinger type equation for the BEC dynamics. The interesting new feature, however, in comparison with earlier settings where such equations emerged including e.g. optical fibers [4,35], is the existence of a variety of external potentials, such as, e.g., a parabolic potential, confining the atoms in a magnetic trap.

The two-dimensional setting of nearly planar (so-called “pancake”) condensates [7] is perhaps especially interesting since it provides the possibility for a variety of rather complex structures, while remaining tractable for computationally demanding, numerical bifurcation/stability studies. Among these structures, we highlight the experimentally realized vortices [42,43] and vortex lattices [3,19] among numerous other theoretically proposed waveforms such as Faraday waves [52], ring dark solitons [53], and soliton/vortex necklaces (see, e.g., [22] for a recent discussion and references therein). For these reasons, it is this two-dimensional context that we aim at addressing herein.

* Corresponding author. Tel.: +1 619 594 7252; fax: +1 619 594 2029.

E-mail addresses: kevrekid@math.umass.edu (P.G. Kevrekidis), carreter@sciences.sdsu.edu (R. Carretero-González).

URLs: <http://www.math.unm.edu/~kapitula> (T. Kapitula), <http://www.rohan.sdsu.edu/~rcarreter> (R. Carretero-González).

¹ URL: <http://nlds.sdsu.edu>.

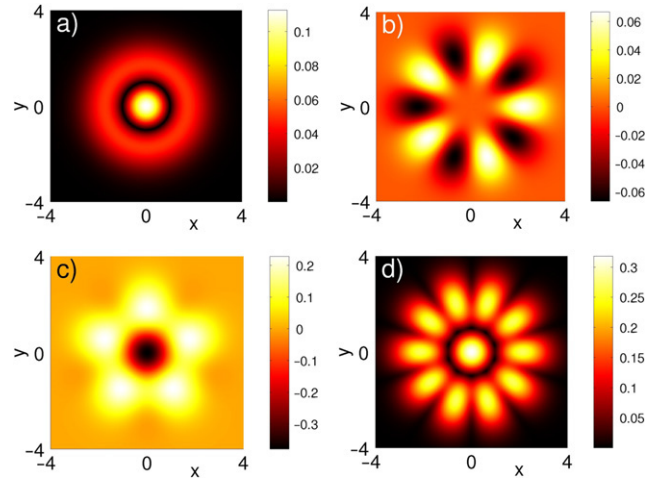


Fig. 1. (Color online) Some of the solutions to Eq. (3.1) when $\ell' = 5$, and for $\Omega = \Omega_{\ell'} (= -6/5)$ given in Eq. (2.6). Panels (a)–(c) correspond to real-valued solutions, whereas panel (d) depicts the modulus of a complex-valued solution. These solutions correspond to: (a) ring, (b) multi-pole, (c) soliton necklace, and (d) vortex necklace.

The governing equation for a two-dimensional Bose–Einstein condensate in a rotating coordinate frame is given by

$$i\partial_t q + \Delta q + \omega q + a|q|^2 q = i\Omega\partial_\theta q + V_{\text{ext}}(\mathbf{x})q, \quad (\partial_\theta := x\partial_y - y\partial_x) \quad (1.1)$$

where $q \in \mathbb{C}$ is the mean-field wavefunction, $a \in \{-1, +1\}$ is the nonlinear interaction ($a = +1$ implies an attractive interaction, whereas $a = -1$ implies a repulsive interaction), $\omega \in \mathbb{R}$ is a free parameter and represents the chemical potential, and $V_{\text{ext}}(\mathbf{x}) : \mathbb{R}^2 \mapsto \mathbb{R}$ represents the trapping potential (see [2,5,8,10,11,29,33,43] and the references therein for further details). The term Ω corresponds to the frequency of the rotation. In this paper it will be assumed that the BEC is subjected to a magnetic trapping potential only, i.e.,

$$V_{\text{ext}}(\mathbf{x}) = |\mathbf{x}|^2. \quad (1.2)$$

The interested reader should consult [1] for a discussion on the validity of Eq. (1.1) as the governing equation in the case of a pancake trap.

Our purpose here will be to determine the existence and linear stability of rotating waves such as ring-like structures, soliton necklaces, vortex necklaces, and the so-called multi-pole states (e.g., quadrupoles and octupoles) in the limit of weak atomic interactions (see Fig. 1). Vortex necklaces have been realized experimentally in [20], and have been discussed from a theoretical and numerical viewpoint in [14,24]. The solutions found in [14] require that the magnetic trap be nonrotating. The multi-pole state given in Eq. (3.9) has been found numerically in [40].

As it will be seen in this text, when considering nonrotating waves, i.e., $\Omega = 0$, the only linearly stable solution of those considered herein is the vortex necklace. For rotating waves whose rotation frequency is

$$\Omega = -2 + 4\frac{1}{\ell}, \quad \ell \in \mathbb{N} \setminus \{1\},$$

it will be seen herein that the ring-like structure is linearly stable for $\ell \geq 6$, and is unstable otherwise. The multi-pole and vortex will continue to be unstable; in fact, as ℓ increases the number of unstable eigenvalues also increases. While the algebraic complexity prevented a calculation for the other two structures, it is suspected that the soliton necklace will continue to be unstable, and the vortex necklace will continue to be stable.

Our exposition will be structured as follows. After determining the spectra of the appropriate linear operator in Section 2 we present the existence theory. The subsequent stability analysis requires two steps: the location of small eigenvalues, and the location of $\mathcal{O}(1)$ eigenvalues with small real part. The analytical results are corroborated in Section 7 by numerical computations. Finally, as a first step in the path towards understanding lattices of the relevant structures, including lattices of vortices constructed experimentally in [3,19], in Section 8 we briefly discuss how one can use these earlier building block solutions to construct multi-ring solutions. We conclude with some final thoughts and open questions.

2. Spectrum for the linear problem

In order to perform the Lyapunov–Schmidt reduction, it is important that one has a thorough understanding of the spectrum $\sigma(\mathcal{L})$ of the associated linear operator, where upon recalling the form of the potential given in Eq. (1.2)

$$\begin{aligned}\mathcal{L} &:= -\Delta + i\Omega\partial_\theta + r^2 \\ &= -\partial_r^2 - \frac{1}{r}\partial_r - \frac{1}{r^2}\partial_\theta^2 + i\Omega\partial_\theta + r^2.\end{aligned}\tag{2.1}$$

If one uses a Fourier decomposition and writes

$$q(r, \theta) = \sum_{\ell=-\infty}^{+\infty} q_\ell(r) e^{i\ell\theta},\tag{2.2}$$

then the eigenvalue problem $\mathcal{L}q = \lambda q$ becomes the infinite sequence of linear Schrödinger eigenvalue problems in the radial variable for $\ell \in \mathbb{Z}$:

$$\mathcal{L}_\ell q_\ell = \lambda q_\ell, \quad \mathcal{L}_\ell := -\partial_r^2 - \frac{1}{r}\partial_r + \frac{\ell^2}{r^2} + r^2 - \ell\Omega.\tag{2.3}$$

Concerning the operator \mathcal{L}_ℓ , it is well known that for each fixed $\ell \in \mathbb{Z}$ there is a countably infinite sequence of simple eigenvalues $\{\lambda_{m,\ell}\}_{m=0}^\infty$, with

$$\lambda_{m,\ell} := 2(|\ell| + 1) + 4m + \ell\Omega,\tag{2.4}$$

such that the eigenfunction $q_{m,\ell}(r)$ corresponding to $\lambda_{m,\ell}$ has precisely m zeros; furthermore, the eigenfunctions do not depend on Ω . With respect to the operator \mathcal{L} , one then has that for each $\lambda_{m,\ell}$ there exist the real-valued eigenfunctions $q_{m,\ell}(r) \cos(\ell\theta)$ and $q_{m,\ell}(r) \sin(\ell\theta)$. This implies that if $\ell \neq 0$, then the eigenvalue is not simple, and has geometric multiplicity no smaller than two. Finally, it is known that if $\lambda \in \sigma(\mathcal{L})$, then $\lambda = \lambda_{m,\ell}$ for some pair $(m, \ell) \in \mathbb{N}_0 \times \mathbb{Z}$. Since $\lambda_{m,\ell} = \lambda_{m',\ell'}$ if and only if

$$\Omega = -2 - 4\frac{m' - m}{\ell' - \ell},\tag{2.5}$$

if $\Omega = 0$ one has that the operator \mathcal{L} has semi-simple eigenvalues with multiplicity greater than two for $m + |\ell| \geq 2$. If $|\Omega| = 2$, then there are an infinite number of eigenvalues with infinite multiplicity; consequently, it will henceforth be assumed that $|\Omega| < 2$ (also see [36, Section 4]).

Assumption 2.1. The rotation frequency Ω satisfies $|\Omega| < 2$.

Without loss of generality, henceforth assume that $\ell \in \mathbb{N}_0$. One of the goals of this paper will be to study the structure of the solutions that arise from eigenvalues of \mathcal{L} having multiplicity three. For example, when $\Omega = 0$ it is clear that $\lambda_{1,0} = \lambda_{0,2} = 6$; furthermore, this eigenvalue has a multiplicity of three. In this paper we will restrict our attention to the case that $\lambda_{1,0} = \lambda_{0,\ell'} = 6$ for some $\ell' \in \mathbb{N}_0$. One sees that this holds when $\Omega = \Omega_{\ell'}$, where

$$\Omega_{\ell'} := -2 + 4\frac{1}{\ell'}.\tag{2.6}$$

Note that $-2 < \Omega_{\ell'} \leq 0$ for $\ell' \geq 2$. Now, when $\Omega = \Omega_{\ell'}$ one has that $\lambda_{m,\ell} = 6$ if and only if

$$\frac{\ell}{\ell'} + m = 1,$$

i.e., $(m, \ell) \in \{(1, 0), (0, \ell')\}$. Thus, for $\Omega = \Omega_{\ell'}$ one has that $\lambda = 6$ is an eigenvalue of multiplicity three for \mathcal{L} ; furthermore, a basis for the eigenspace is given by $\ker(\mathcal{L} - 6) = \text{Span}\{q_{1,0}(r), q_{0,\ell'} \cos \ell'\theta, q_{0,\ell'} \sin \ell'\theta\}$.

Proposition 2.2. *Suppose that $\ell' \in \mathbb{N} \setminus \{1\}$. When $\Omega = \Omega_{\ell'}$, where $\Omega_{\ell'}$ is given in Eq. (2.6), one has that $\lambda = 6$ is an eigenvalue of \mathcal{L} with geometric multiplicity three. Furthermore,*

$$\ker(\mathcal{L} - 6) = \text{Span}\{q_{1,0}(r), q_{0,\ell'} \cos \ell'\theta, q_{0,\ell'} \sin \ell'\theta\}.$$

Remark 2.3. There are two principal reasons as to why we focus on the case $\Omega = \Omega_{\ell'}$ in this paper:

- From a mathematical perspective, the solution structure associated with multiplicity three eigenvalues is much richer than that for multiplicity two eigenvalues; however, the bifurcation equations are still analytically tractable.
- From a physical perspective, structures pertaining to different discrete rotation frequencies are of interest. While lower such frequencies have been explored numerically [31,49] and experimentally [51], recent optical techniques [17,18] render even higher such frequencies potentially accessible to the experiment.

3. Existence

3.1. Lyapunov–Schmidt reduction

For some $\ell' \geq 2$, set $\Omega = \Omega_{\ell'}$, where $\Omega_{\ell'}$ is given in Eq. (2.6). Rewrite the steady-state problem associated with Eq. (1.1) as

$$\mathcal{L}_{\ell'} q - \omega q - a|q|^2 q = 0, \tag{3.1}$$

where the operator $\mathcal{L}_{\ell'}$ is given in Eq. (2.3). Using the result of Proposition 2.2, write

$$q = (x_1 q_{1,0}(r) + y_1 q_{0,\ell'}(r) \cos \ell' \theta + y_2 q_{0,\ell'}(r) \sin \ell' \theta) \epsilon^{1/2} + \mathcal{O}(\epsilon), \quad \omega = 6 + \Delta \omega \epsilon + \mathcal{O}(\epsilon^{3/2}), \tag{3.2}$$

where $x_1, y_1, y_2 \in \mathbb{C}$. Now, Eq. (3.1) is invariant under the gauge symmetry $q \mapsto q e^{i\phi}$, and under the spatial SO(2) symmetry of rotation. The equivariant Lyapunov–Schmidt bifurcation theory guarantees that the bifurcation equations have the same symmetries as the underlying system (e.g., see [13]). Consequently, without loss of generality one may assume in Eq. (3.2) that $x_1 \in \mathbb{R}$ and $y_2 \in i\mathbb{R}$. Upon doing so Eq. (3.2) becomes

$$q = (x_1 q_{1,0}(r) + y_1 q_{0,\ell'}(r) \cos \ell' \theta + i y_2 q_{0,\ell'}(r) \sin \ell' \theta) \epsilon^{1/2} + \mathcal{O}(\epsilon), \quad \omega = 6 + \Delta \omega \epsilon + \mathcal{O}(\epsilon^{3/2}), \tag{3.3}$$

where now one has that $x_1, y_2 \in \mathbb{R}$, and $y_1 \in \mathbb{C}$.

It is now time to perform the Lyapunov–Schmidt reduction. First, an explicit calculation yields that

$$q_{1,0}(r) = \sqrt{\frac{1}{\pi}} (1 - r^2) e^{-r^2/2}, \quad q_{0,\ell'}(r) = \sqrt{\frac{2}{\ell'! \pi}} r^{\ell'} e^{-r^2/2}. \tag{3.4}$$

Set

$$\begin{aligned} g_0 &:= \int_0^\infty r q_{1,0}^4(r) dr = \frac{1}{8} \frac{1}{\pi^2} \\ g_{\ell'} &:= \int_0^\infty r q_{0,\ell'}^4(r) dr = \frac{(2\ell')!}{4^{\ell'} (\ell'!)^2} \frac{1}{\pi^2} \\ g_{0\ell'} &:= \int_0^\infty r q_{1,0}^2(r) q_{0,\ell'}^2(r) dr = \frac{\ell'^2 - \ell' + 2}{2^{\ell'+3}} \frac{1}{\pi^2}, \end{aligned} \tag{3.5}$$

and note that the evaluations of the integrals in Eq. (3.5) are possible as a result of Eq. (3.4). Further set

$$\mu := \frac{a \Delta \omega}{g_0 \pi}, \quad g_1 := \frac{g_{0\ell'}}{g_0}, \quad g_2 := \frac{g_{0\ell'}}{g_{\ell'}}, \quad c_g := \frac{g_2}{g_1}, \tag{3.6}$$

and note that explicit representations of these quantities are available via Eq. (3.5). Substitution of Eq. (3.3) into Eq. (3.1), applying the Lyapunov–Schmidt reduction, and using the definitions in Eq. (3.6) yield the bifurcation equations:

$$\begin{aligned} 0 &= x_1 \left[\mu + 2x_1^2 + g_1(2|y_1|^2 + y_1^2 + y_2^2) \right] \\ 0 &= c_g \mu y_1 + g_2 x_1^2 (2y_1 + y_1^*) + \frac{3}{4} |y_1|^2 y_1 + \frac{1}{4} y_2^2 (2y_1 - y_1^*) \\ 0 &= y_2 \left[c_g \mu + g_2 x_1^2 + \frac{1}{4} (2|y_1|^2 - y_1^2) + \frac{3}{4} y_2^2 \right]. \end{aligned} \tag{3.7}$$

The zero set of Eq. (3.7) will be studied in the next two subsections.

3.2. Real-valued solutions

When considering real-valued solutions to Eq. (3.1), one must assume in Eq. (3.7) that $y_2 = 0$ and $y_1 \in \mathbb{R}$. Upon doing so Eq. (3.7) becomes the reduced system:

$$\begin{aligned} 0 &= x_1 \left[\mu + 2x_1^2 + 3g_1 y_1^2 \right] \\ 0 &= y_1 \left[c_g \mu + 3g_2 x_1^2 + \frac{3}{4} y_1^2 \right]. \end{aligned} \tag{3.8}$$

There are three solutions to Eq. (3.8): the pure mode solutions (that will be called, respectively, the ring and multi-pole solutions in what follows),

$$\begin{pmatrix} x_1^2 \\ y_1^2 \end{pmatrix} = -\frac{1}{2}\mu \begin{pmatrix} 1 \\ 0 \end{pmatrix}, \quad \begin{pmatrix} x_1^2 \\ y_1^2 \end{pmatrix} = -\frac{4}{3}c_g\mu \begin{pmatrix} 0 \\ 1 \end{pmatrix}, \tag{3.9}$$

and what will henceforth be termed the *soliton necklace* solution,

$$\begin{pmatrix} x_1^2 \\ y_1^2 \end{pmatrix} = -\frac{2\mu}{3(1-6g_1g_2)} \begin{pmatrix} 3(1/4-g_2) \\ 3c_g(2/3-g_1) \end{pmatrix}. \tag{3.10}$$

In order for the solution in Eq. (3.10) to be valid, one must have that $(1/4 - g_2)(2/3 - g_1) > 0$. It can be checked numerically via the use of Eq. (3.6) that this inequality holds for all $\ell' \in \mathbb{N} \setminus \{1, 6\}$ (recall that we are assuming that $\ell' \geq 2$). Furthermore, for all of the solutions given above one must have that $\mu < 0$, i.e., $\text{sign}(a\Delta\omega) < 0$.

Lemma 3.1. *There are three distinct real-valued solutions to Eq. (3.1). The pure mode solutions, i.e., the ring and the multi-pole, are given by*

$$q \sim x_1q_{1,0}(r)\epsilon^{1/2}, \quad q \sim y_1q_{0,\ell'}(r)\cos(\ell'\theta)\epsilon^{1/2},$$

respectively, where x_1, y_1 are given in Eq. (3.9). The soliton necklace solution is given by

$$q \sim (x_1q_{1,0}(r) + y_1q_{0,\ell'}(r)\cos(\ell'\theta))\epsilon^{1/2},$$

where the pair (x_1, y_1) is given in Eq. (3.10). The soliton necklace solution exists for all $\ell' \in \mathbb{N} \setminus \{1, 6\}$. Finally, all of the solutions require that $a\Delta\omega \in \mathbb{R}^-$. See Fig. 1.

Remark 3.2. It is open question as to why the soliton necklace does not exist for $\ell' = 6$ ($\Omega = \Omega_6 = -4/3$). It does appear as if this rotation frequency is unique in some as yet undetermined way. As it will be seen in Section 5 (in particular, see Eq. (5.2)), there is a stability transition between $\ell' = 5$ and $\ell' = 7$. Furthermore, it is seen in Lemma 3.3 that there is a complex-valued solution which exists only when $\ell' = 6$.

3.3. Complex-valued solutions

Now let us find complex-valued solutions to Eq. (3.1). Upon setting $y_1 := se^{i\psi}$, where $s \in \mathbb{R}^+$, Eq. (3.7) becomes

$$\begin{aligned} 0 &= x_1 \left[\mu + 2x_1^2 + g_1((2 + e^{i2\psi})s^2 + y_2^2) \right] \\ 0 &= s \left[c_g\mu + g_2(2 + e^{-i2\psi})x_1^2 + \frac{3}{4}s^2 + \frac{1}{4}(2 - e^{-i2\psi})y_2^2 \right] \\ 0 &= y_2 \left[c_g\mu + g_2x_1^2 + \frac{1}{4}(2 - e^{i2\psi})s^2 + \frac{3}{4}y_2^2 \right]. \end{aligned} \tag{3.11}$$

Note that Eq. (3.11) requires that $(x_1, s, y_2) \in \mathbb{R} \times \mathbb{R}^+ \times \mathbb{R}$, and further note that the imaginary part of Eq. (3.11) satisfies the system

$$s^2 \sin 2\psi = 0, \quad \left(g_2x_1^2 - \frac{1}{4}y_2^2 \right) \sin 2\psi = 0. \tag{3.12}$$

First suppose that $s = 0$, so that Eq. (3.11) collapses to

$$\begin{aligned} 0 &= x_1 \left[\mu + 2x_1^2 + g_1y_2^2 \right] \\ 0 &= y_2 \left[c_g\mu + g_2x_1^2 + \frac{3}{4}y_2^2 \right]. \end{aligned} \tag{3.13}$$

The only solution not already considered in Section 3.2 is given by what will henceforth be called a *vortex necklace*,

$$\begin{pmatrix} x_1^2 \\ y_2^2 \end{pmatrix} = -\frac{2\mu}{3-2g_1g_2} \begin{pmatrix} 3/4-g_2 \\ c_g(2-g_1) \end{pmatrix}. \tag{3.14}$$

In order for the solution in Eq. (3.14) to be valid one must have that $(3/4 - g_2)(2 - g_1) > 0$. It can be checked numerically via the use of Eq. (3.6) that this inequality holds for all $\ell' \in \mathbb{N} \setminus \{1\}$. Furthermore, for the solution in Eq. (3.14) to be valid one must again have that $\mu < 0$.

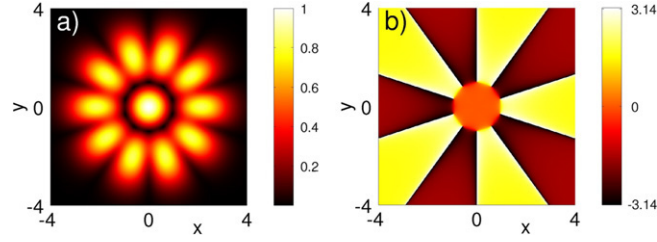


Fig. 2. (Color online) The vortex necklace solution to Eq. (3.1) when $\ell' = 5$ (see panel (d) in Fig. 1). Panel (a) depicts the modulus of the solution, and panel (b) its phase.

Now suppose that $s \neq 0$, which by Eq. (3.12) necessarily implies that $\psi = 0 \pmod{\pi/2}$. Under this restriction the real part of Eq. (3.11) becomes

$$\begin{aligned} 0 &= x_1 \left[\mu + 2x_1^2 + g_1((2 + \cos 2\psi)s^2 + y_2^2) \right] \\ 0 &= s \left[c_g \mu + g_2(2 + \cos 2\psi)x_1^2 + \frac{3}{4}s^2 + \frac{1}{4}(2 - \cos 2\psi)y_2^2 \right] \\ 0 &= y_2 \left[c_g \mu + g_2x_1^2 + \frac{1}{4}(2 - \cos 2\psi)s^2 + \frac{3}{4}y_2^2 \right]. \end{aligned} \tag{3.15}$$

Recall that the goal is to find solutions not already found in Section 3.2. The radially symmetric vortex solution is given by $\psi = 0 \pmod{\pi}$ with

$$x_1 = 0, \quad \begin{pmatrix} s^2 \\ y_2^2 \end{pmatrix} = -c_g \mu \begin{pmatrix} 1 \\ 1 \end{pmatrix}. \tag{3.16}$$

Now, suppose that all the variables in Eq. (3.15) are to be nonzero. If $\psi = \pi/2 \pmod{\pi}$, then by the SO(2) spatial symmetry the solution to be found is equivalent to that given in Eq. (3.14). Hence, finally assume that $\psi = 0 \pmod{\pi}$. In this case the solution is given by

$$\begin{pmatrix} x_1^2 \\ s^2 \\ y_2^2 \end{pmatrix} = -\frac{\mu}{2(6g_1g_2 - 1)} \begin{pmatrix} 1 - 4g_2 \\ c_g(-2 + 4g_1 - 4g_1g_2) \\ 2c_g(6g_1g_2 - 1) \end{pmatrix}. \tag{3.17}$$

A straightforward computation using Eq. (3.6) shows that the solution in Eq. (3.17) is valid if and only if $\ell' = 6$. It is extremely interesting to note that this is complementary to those values of ℓ' for which the soliton necklace given in Eq. (3.10) exists.

Lemma 3.3. *There are three distinct complex-valued solutions to Eq. (3.1). The radially symmetric vortex is given by*

$$q \sim y_2 q_{0,\ell'}(r) e^{i\ell'\theta} \epsilon^{1/2},$$

where y_2 is given in Eq. (3.16). The vortex necklace solution is given by

$$q \sim (x_1 q_{1,0}(r) + i y_2 q_{0,\ell'}(r) \sin(\ell'\theta)) \epsilon^{1/2},$$

where the pair (x_1, y_2) is given in Eq. (3.14). Finally, for $\ell' = 6$ there exists an additional solution which is given by

$$q \sim (x_1 q_{1,0}(r) + s q_{0,\ell'}(r) \cos(\ell'\theta) + i y_2 q_{0,\ell'}(r) \sin(\ell'\theta)) \epsilon^{1/2},$$

where the triple (x_1, s, y_2) is given in Eq. (3.17). All of the solutions require that $a\Delta\omega \in \mathbb{R}^-$. See Figs. 1 and 2.

4. Stability: Preliminary discussion

The theory leading to the determination of the spectral stability of the solutions found in Section 3 will depend upon the results presented in [28, Section 4] and [26,27,46]. Upon taking real and imaginary parts via $q := u + iv$, and linearizing Eq. (1.1) about a complex-valued solution $Q = U + iV$, one has the eigenvalue problem

$$J\mathcal{L}u = \lambda u, \tag{4.1}$$

where

$$J := \begin{pmatrix} 0 & 1 \\ -1 & 0 \end{pmatrix}, \quad \mathcal{L} := (\mathcal{L}_{\ell'} - \omega)\mathbb{1} - a \begin{pmatrix} 3U^2 + V^2 & 2UV \\ 2UV & U^2 + 3V^2 \end{pmatrix}.$$

For Eq. (4.1) let k_r represent the number of real positive eigenvalues, k_c the number of eigenvalues in the open first quadrant of the complex plane, and $k_i^-(k_i^+)$ the number of purely imaginary eigenvalues with positive imaginary part and negative (positive) Krein sign. The Krein signature of a simple eigenvalue $\lambda \in i\mathbb{R}^+$ is given by

$$K := \text{sign}(\langle \text{Re}(\mathbf{u}_\lambda), \mathcal{L}\text{Re}(\mathbf{u}_\lambda) \rangle), \quad (4.2)$$

where the associated eigenfunction of Eq. (4.1) is given by \mathbf{u}_λ (see [26, Section 2.2] and [23, Section 2] for more details). In Eq. (4.2) $\langle \cdot, \cdot \rangle$ refers to the inner product on an appropriate Hilbert space.

Let $n(\mathcal{L})$ correspond to the number of negative eigenvalues of the symmetric operator \mathcal{L} (finite as a consequence of Assumption 2.1), and let $z(\mathcal{L}) = \dim(\ker(\mathcal{L}))$. Suppose that $z(\mathcal{L}) = k$ with an orthonormal basis for $\ker(\mathcal{L})$ being given by $\ker(\mathcal{L}) = \text{Span}\{\phi_1, \dots, \phi_k\}$. For $j = 1, \dots, k$ let ψ_j be defined by $\mathbf{J}\mathcal{L}\psi_j = \phi_j$. The existence of the generalized eigenfunctions is guaranteed by the facts that (a) the operator $\mathbf{J}\mathcal{L}$ corresponds to the linearization of a Hamiltonian system, and (b) the null space of \mathcal{L} is generated by the group symmetries associated with the Hamiltonian system (e.g., see [26, Section 2.1]). The result of [27] states that

$$k_r + 2k_i^- + 2k_c = n(\mathcal{L}) - n(\mathbf{D}), \quad (4.3)$$

where

$$\mathbf{D}_{ij} := \langle \psi_i, \mathcal{L}\psi_j \rangle, \quad i, j = 1, \dots, k. \quad (4.4)$$

If the underlying solution is real-valued, i.e., $V \equiv 0$, then Eq. (4.3) can be refined. In this case set

$$L_+ := \mathcal{L}_{\ell'} - \omega - 3aU^2, \quad L_- := \mathcal{L}_{\ell'} - \omega - aU^2, \quad (4.5)$$

so that Eq. (4.1) becomes

$$L_+u = -\lambda v, \quad L_-v = \lambda u. \quad (4.6)$$

Suppose that

$$\ker(L_\pm) = \text{Span}\{\phi_1^\pm, \dots, \phi_{k_\pm}^\pm\}, \quad k_- + k_+ = k,$$

and further suppose that

$$L_+\psi_j^- = -\phi_j^-, \quad (j = 1, \dots, k_-); \quad L_-\psi_j^+ = \phi_j^+, \quad (j = 1, \dots, k_+).$$

One then has that $\mathbf{D} = \text{diag}(\mathbf{D}_+, \mathbf{D}_-)$, with

$$(\mathbf{D}_\pm)_{ij} := \langle \psi_i^\mp, L_\pm \psi_j^\mp \rangle, \quad (4.7)$$

and Eq. (4.3) can be rewritten as

$$k_r + 2k_i^- + 2k_c = [n(L_+) - n(\mathbf{D}_+)] + [n(L_-) - n(\mathbf{D}_-)]. \quad (4.8)$$

Furthermore, one has the lower bound

$$k_r \geq |[n(L_+) - n(\mathbf{D}_+)] - [n(L_-) - n(\mathbf{D}_-)]|. \quad (4.9)$$

Now consider the solutions described in Section 3. Since $U, V = \mathcal{O}(\sqrt{\epsilon})$, one has that in Eq. (4.1)

$$\mathcal{L} = (\mathcal{L}_{\ell'} - 6)\mathbb{1} + \mathcal{O}(\epsilon).$$

The fact that $z((\mathcal{L}_{\ell'} - 6)\mathbb{1}) = 6$ implies that for Eq. (4.1) there will be six eigenvalues of $\mathcal{O}(\epsilon)$. Some of these eigenvalues will remain at the origin due to the symmetries present in Eq. (1.1). Unfortunately, the perturbation calculations presented in Section 5 will be insufficient to fully determine the spectral stability of the solutions, as they describe only those eigenvalues for Eq. (4.1) of $\mathcal{O}(\epsilon)$. It is possible that $\mathcal{O}(1)$ eigenvalues of opposite sign collide, and hence create a so-called oscillatory instability associated with a complex eigenvalue. This issue will be considered in Section 6.

5. Stability: Small eigenvalues

There are two conserved quantities associated with Eq. (1.1) which are a consequence of symmetry:

$$N := \iint_{\mathbb{R}^2} |q(\mathbf{x})|^2 \, d\mathbf{x}; \quad L_z := - \iint_{\mathbb{R}^2} \text{Im}(q(\mathbf{x})) \partial_\theta \text{Re}(q(\mathbf{x})) \, d\mathbf{x},$$

where $\partial_\theta := x\partial_y - y\partial_x$. The quantity N refers to the number of particles, while L_z refers to the total angular momentum of the condensate. Consequently, for the linearized problem one typically has that $\lambda = 0$ is an eigenvalue with some multiplicity. When discussing the solutions found in Section 3, one has the following table regarding the multiplicity of the null eigenvalue:

Solution type	geometric multiplicity	algebraic multiplicity
radially symmetric moduli	1	2
not radially symmetric moduli	2	4

(5.1)

The disparity is due to the fact that the null eigenfunctions associated with N and L_z are constant multiples of each other for solutions of the form $q(r)e^{i\ell\theta}$, i.e., solutions with radially symmetric moduli. It is interesting to note that the radially symmetric solutions do not have the maximal geometric multiplicity.

Regarding the nonzero eigenvalues of $\mathcal{O}(\epsilon)$, the table in Eq. (5.2) summarizes the calculations of the next subsection. Since $k_c = 0$ in all cases, this quantity has not been included therein. If $a = +1$, then in Eq. (5.2) one should interchange the entries associated with k_i^+ and k_i^- . Note that for all solutions except for the soliton necklace one has that as ℓ' increases, i.e., as $\Omega_{\ell'} \rightarrow -2^+$, the wave stabilizes (at least with respect to the small eigenvalues).

Solution	$a = -1$ (repulsive)								
	$2 \leq \ell' \leq 5$			$\ell' = 6$			$\ell' \geq 7$		
	k_r	k_i^-	k_i^+	k_r	k_i^-	k_i^+	k_r	k_i^-	k_i^+
<i>ring</i>	2	0	0	0	2	0	0	2	0
<i>multi-pole</i>	1	0	0	1	0	0	0	1	0
<i>soliton necklace</i>	0	1	0				1	0	0
<i>vortex</i>	0	0	2	0	0	2	0	1	1
<i>vortex necklace</i>	0	1	0	0	1	0	0	1	0

(5.2)

Remark 5.1. Recall from Lemma 3.1 that the soliton necklace does not exist for $\ell' = 6$. Since the solution given in Eq. (3.17) exists only for $\ell' = 6$, i.e., a distinguished rotation frequency, we chose not to determine its stability herein. However, the interested reader can use the subsequent analysis in order to make this determination.

5.1. Reduced eigenvalue problem: Theory

Consider a general form of Eq. (4.1) under the following scenario:

$$J := \begin{pmatrix} \mathbf{0} & \mathbb{1} \\ -\mathbb{1} & \mathbf{0} \end{pmatrix}, \quad \mathcal{L} = \mathcal{L}_0 + \epsilon\mathcal{L}_1,$$

with

$$\mathcal{L}_0 := \text{diag}(A_0, A_0), \quad \mathcal{L}_1 := \begin{pmatrix} L_+^1 & B \\ B & L_-^1 \end{pmatrix}. \tag{5.3}$$

Here it is assumed that $0 < \epsilon \ll 1$, and that the operators A_0 , L_\pm^1 , and B are self-adjoint on a Hilbert space X with inner product $\langle \cdot, \cdot \rangle$. Furthermore, it will be assumed that the operators satisfy the assumptions given in [26, Section 2]; in particular, they are relatively compact perturbations of self-adjoint and strictly positive operators.

Assume that $z(A_0) = n \in \mathbb{N}$, and that the orthonormal basis for $\ker(A_0)$ is given by

$$\ker(A_0) = \text{Span}\{\phi_1, \dots, \phi_n\}. \tag{5.4}$$

As seen in [28, Section 4], upon writing

$$\lambda = \epsilon\lambda_1 + \mathcal{O}(\epsilon^2), \quad u = \sum_{j=1}^n x_j(\phi_j, 0)^T + \sum_{j=1}^n x_{n+j}(0, \phi_j)^T + \mathcal{O}(\epsilon),$$

the determination of the $\mathcal{O}(\epsilon)$ eigenvalues to Eq. (5.3) is equivalent to the finite-dimensional eigenvalue problem

$$JSx = \lambda_1 x; \quad J := \begin{pmatrix} \mathbf{0} & \mathbb{1} \\ -\mathbb{1} & \mathbf{0} \end{pmatrix}, \quad S := \begin{pmatrix} S_+ & S_2 \\ S_2 & S_- \end{pmatrix}, \tag{5.5}$$

where

$$(\mathbf{S}_\pm)_{ij} = \langle \phi_i, L_\pm^1 \phi_j \rangle, \quad (\mathbf{S}_2)_{ij} = \langle \phi_i, B \phi_j \rangle. \tag{5.6}$$

Now consider the special case that $B = 0$. Eq. (5.5) then reduces to

$$\mathbf{S}_+ \mathbf{u} = -\lambda_1 \mathbf{v}, \quad \mathbf{S}_- \mathbf{v} = \lambda_1 \mathbf{u}, \tag{5.7}$$

which can be rewritten as the system

$$\mathbf{S}_+ \mathbf{S}_- \mathbf{v} = -\lambda_1^2 \mathbf{v}. \tag{5.8}$$

For the perturbed problem suppose that $z(L_\pm) = n_\pm$, where $0 \leq n_\pm \leq n$. One then has the existence of two orthonormal bases for $\ker(\mathbf{S}_\pm)$, say

$$\ker(\mathbf{S}_\pm) = \text{Span}\{\mathbf{a}_1^\pm, \dots, \mathbf{a}_{n_\pm}^\pm\}.$$

Now let \mathbf{b}_j^\pm be such that

$$\mathbf{S}_+ \mathbf{b}_j^- = -\mathbf{a}_j^-, \quad (j = 1, \dots, n_-); \quad \mathbf{S}_- \mathbf{b}_j^+ = \mathbf{a}_j^+, \quad (j = 1, \dots, n_+).$$

Following [26, Section 3.3] one has that the \mathbf{D}_\pm given in Eq. (4.7) are to leading order

$$(\mathbf{D}_\pm)_{ij} = \langle \mathbf{b}_i^\mp, \mathbf{S}_\pm \mathbf{b}_j^\mp \rangle. \tag{5.9}$$

Consequently, when considering the eigenvalues of $\mathcal{O}(\epsilon)$ one can rewrite Eqs. (4.8) and (4.9) as

$$\begin{aligned} k_r + 2k_1^- + 2k_c &= [n(\mathbf{S}_+) - n(\mathbf{D}_+)] + [n(\mathbf{S}_-) - n(\mathbf{D}_-)] \\ k_r &\geq |[n(\mathbf{S}_+) - n(\mathbf{D}_+)] - [n(\mathbf{S}_-) - n(\mathbf{D}_-)]|. \end{aligned} \tag{5.10}$$

Remark 5.2. Since Eq. (5.7) describes a finite-dimensional system, one also has that

$$k_r + 2k_1^+ + 2k_c = [p(\mathbf{S}_+) - p(\mathbf{D}_+)] + [p(\mathbf{S}_-) - p(\mathbf{D}_-)],$$

where k_1^+ represents the number of purely imaginary eigenvalues with positive imaginary part and positive Krein sign. Here $p(\mathbf{A})$ refers to the number of positive eigenvalues for the symmetric matrix \mathbf{A} .

5.2. Reduced eigenvalue problem: Real-valued solutions

Recall Eqs. (4.6) and (5.3). In this case one has $B = 0$ with

$$L_+^1 = -\Delta\omega - 3aU^2, \quad L_-^1 = -\Delta\omega - aU^2,$$

where $U\epsilon^{-1/2}$ is given in Lemma 3.1 for each solution under consideration. Following the notation in Eq. (5.4), for $j = 1, \dots, 3$ write

$$\phi_1 := q_{1,0}(r), \quad \phi_2 := q_{0,\ell'}(r) \cos(\ell'\theta), \quad \phi_3 := q_{0,\ell'}(r) \sin(\ell'\theta).$$

Consider the first solution given in Eq. (3.9), i.e., the radially symmetric ring which satisfies $\mu + 2ax_1^2 = 0$. Recall that as a consequence of Eq. (5.1) there will be four nonzero eigenvalues of $\mathcal{O}(\epsilon)$. Upon using Eq. (5.6) one eventually sees that

$$\mathbf{S}_+ = -g_0\pi ax_1^2 \text{diag}(4, 3g_1 - 2, 3g_1 - 2), \quad \mathbf{S}_- = -g_0\pi ax_1^2 \text{diag}(0, g_1 - 2, g_1 - 2). \tag{5.11}$$

Upon following the reasoning leading to Eq. (5.9) one has that $\mathbf{D} = \mathbf{D}_+$ with

$$\mathbf{D}_+ = \left(-\frac{1}{4g_0ax_1^2} \right) \implies n(\mathbf{D}_+) = \begin{cases} 0, & a = -1 \\ 1, & a = +1. \end{cases} \tag{5.12}$$

Upon using Eq. (3.6) one has that $g_1 < 2$ for all $\ell' \geq 2$, whereas $g_1 - 2/3 > 0$ for $\ell' = 2, \dots, 5$, and is negative otherwise. Finally, for the matrices given in Eq. (5.11) the eigenvalue problem of Eq. (5.7) is particularly easy to solve, and one sees that the nonzero eigenvalues are given by

$$\lambda_1^2 = -(g_0\pi ax_1^2)^2 (g_1 - 2)(3g_1 - 2). \tag{5.13}$$

If $\ell' = 2, \dots, 5$ then to leading order the two nonzero eigenvalues in the closed right half of the complex plane are semi-simple with multiplicity two; furthermore, by Eq. (5.13) one clearly sees that $k_r = 2$. When $\epsilon = 0$ one has that $n(L_+) = n(L_-)$, so that for $\epsilon > 0$ sufficiently small one has that

$$|n(L_+) - n(L_-)| = |[n(S_+) - n(D_+)] - n(S_-)| = 2.$$

As a consequence of Eq. (4.9) one can then conclude that $k_r = 2$ to all orders in the perturbation expansion.

If $\ell' \geq 6$, and if $a = -1$, then by applying Eq. (5.10) and Remark 5.2 one has that

$$k_i^- + k_c = 2, \quad k_i^+ + k_c = 0;$$

thus, $k_i^- = 2$ and $k_c = 0$. If $a = +1$, then the conclusion is that $k_i^+ = 2$. In either case, as a consequence of [23, Lemma 2.10] one has that the quadratic form $\langle \mathcal{L}u, u \rangle$ restricted to the four-dimensional invariant subspace associated with the eigenvalues $\pm i[\lambda_1 \epsilon + \mathcal{O}(\epsilon^2)]$ is either positive definite ($a = +1$) or negative definite ($a = -1$) for $\epsilon > 0$ sufficiently small. If $k_c = 1$, then this quadratic form would have two positive directions and two negative directions (again see [23, Lemma 2.10]). Consequently, one can conclude that the eigenvalues remain purely imaginary to all orders in the perturbation expansion.

Now consider the second solution given in Eq. (3.9), i.e., the multi-pole solution which satisfies $c_g \mu + 3ay_1^2/4 = 0$. In this case referencing Eq. (5.1) yields that there will be only two nonzero eigenvalues of $\mathcal{O}(\epsilon)$. Upon using Eq. (5.6) one eventually sees that

$$S_+ = -g_{\ell'} \pi a y_1^2 \text{diag} \left(3g_2 - \frac{3}{4}, \frac{3}{2}, 0 \right), \quad S_- = -g_{\ell'} \pi a y_1^2 \text{diag} \left(g_2 - \frac{3}{4}, 0, -\frac{1}{2} \right). \quad (5.14)$$

Regarding D , one has a similar conclusion as that given in Eq. (5.12). Upon using Eq. (3.6) one has that $g_2 < 3/4$ for all $\ell' \geq 2$, whereas $g_2 - 1/4 > 0$ for $\ell' = 2, \dots, 6$, and is negative otherwise. Finally, for the matrices given in Eq. (5.14) the eigenvalue problem of Eq. (5.7) is particularly easy to solve, and one sees that the nonzero eigenvalue in the closed right half of the plane is given by

$$\lambda_1^2 = -3(g_{\ell'} \pi a y_1^2)^2 \left(g_2 - \frac{1}{4} \right) \left(g_2 - \frac{3}{4} \right). \quad (5.15)$$

By Eq. (5.15) one clearly sees that to leading order $k_r = 1$ for $\ell' = 2, \dots, 6$. If $\ell' \geq 7$, then by arguing as in the previous paragraph one has that

$$k_i^- = \begin{cases} 1, & a = -1 \\ 0, & a = +1 \end{cases}, \quad k_i^+ = 1 - k_i^-.$$

Finally, consider the solution given in Eq. (3.10), i.e., the soliton necklace. Upon using Eq. (5.6) one eventually sees that

$$S_+ = -2g_0 g_1 \pi a \begin{pmatrix} 2x_1^2/g_2 & 3x_1 y_1 & 0 \\ 3x_1 y_1 & 3y_1^2/4g_2 & 0 \\ 0 & 0 & 0 \end{pmatrix}, \quad S_- = -2g_0 g_1 \pi a \begin{pmatrix} -y_1^2 & x_1 y_1 & 0 \\ x_1 y_1 & -x_1^2 & 0 \\ 0 & 0 & -x_1^2 - y_1^2/4g_2 \end{pmatrix}. \quad (5.16)$$

Upon using Eq. (5.8) it is seen that the eigenvalue in the closed right half of the plane is given by

$$\begin{aligned} \lambda^2 &= -\text{trace}(S_+ S_-) \\ &= -(2\pi g_0 g_1 x_1 y_1)^2 \left(6 - \frac{2}{g_1} - \frac{3}{4g_2} \right). \end{aligned} \quad (5.17)$$

Upon using Eq. (3.6) one sees that $\lambda^2 \in \mathbb{R}^-$ for $\ell' = 2, \dots, 5$, whereas $\lambda^2 \in \mathbb{R}^+$ for $\ell' \geq 7$ (recall that the solution does not exist for $\ell' = 6$). If $\ell' = 2, \dots, 5$, then arguing as above for the multi-mode solution yields that

$$k_i^- = \begin{cases} 1, & a = -1 \\ 0, & a = +1 \end{cases}, \quad k_i^+ = 1 - k_i^-.$$

5.3. Reduced eigenvalue problem: Complex-valued solutions

Here one has that

$$L_+^1 = -\Delta\omega - a(3U^2 + V^2), \quad L_-^1 = -\Delta\omega - a(U^2 + 3V^2), \quad B = -2aUV. \quad (5.18)$$

The explicit form of $U\epsilon^{-1/2}$ and $V\epsilon^{-1/2}$ can be deduced from Lemma 3.3.

First consider the vortex necklace solution given in Eq. (3.14). One eventually sees that for Eq. (5.5),

$$\mathbf{S}_+ = -2g_0g_1\pi a \operatorname{diag} \left(2x_1^2/g_1, x_1^2, x_1^2 - y_1^2/4g_2 \right), \quad \mathbf{S}_- = -2g_0g_1\pi a \operatorname{diag} \left(y_1^2, 3y_1^2/4g_2, 0 \right)$$

$$\mathbf{S}_2 = -2g_0g_1\pi a \begin{pmatrix} 0 & x_1y_1 & 0 \\ x_1y_1 & 0 & 0 \\ 0 & 0 & 0 \end{pmatrix}.$$

Using the above formulation, one sees that for Eq. (5.5) the subspace $\operatorname{Span}(\{\mathbf{e}_3, \mathbf{e}_6\})$ is invariant; furthermore, the eigenvalue associated with this subspace is $\lambda_1 = 0$. Upon reordering the remaining basis vectors via the mapping

$$\{\mathbf{e}_1, \mathbf{e}_2, \mathbf{e}_4, \mathbf{e}_5\} \mapsto \{\mathbf{e}_2, \mathbf{e}_4, \mathbf{e}_1, \mathbf{e}_5\}, \quad (5.19)$$

one sees that the remaining eigenvalues for Eq. (5.5) can be found via solving $\mathbf{AB}\mathbf{x} = \lambda_1^2\mathbf{x}$, where

$$\mathbf{A} := -2g_0g_1\pi a \begin{pmatrix} x_1y_1 & 3y_1^2/4g_2 \\ -2x_1^2/g_1 & -x_1y_1 \end{pmatrix}, \quad \mathbf{B} := -2g_0g_1\pi a \begin{pmatrix} x_1y_1 & y_1^2 \\ -x_1^2 & -x_1y_1 \end{pmatrix}. \quad (5.20)$$

Now, the nonzero eigenvalue in the closed right half of the plane for Eq. (5.20) is given by

$$\lambda_1^2 = \operatorname{trace}(\mathbf{AB})$$

$$= (2\pi g_0g_1x_1y_1)^2 \left(2 - \frac{2}{g_1} - \frac{3}{4g_2} \right). \quad (5.21)$$

Upon using Eq. (3.6) one sees that $\lambda_1^2 \in \mathbb{R}^-$ for $\ell' \geq 2$; hence, the wave is spectrally stable.

In order to determine the signature of the nonzero eigenvalue, one must compute $\sigma(\mathbf{S})$ (note that $z(\mathbf{S}) = 2$) and use Eq. (4.3). Proceeding in a manner similar to that above, and using the fact that

$$3 - 2g_1g_2 \in \mathbb{R}^+, \quad 1 - g_2 - \frac{1}{2g_1} \in \begin{cases} \mathbb{R}^+, & \ell' = 2, \dots, 4 \\ \mathbb{R}^-, & \ell' \geq 5, \end{cases}$$

one eventually sees that

	$\ell' = 2, \dots, 4$	$\ell' \geq 5$
$a = -1$	$n(\mathbf{S}) = 4$	$n(\mathbf{S}) = 3$
$a = +1$	$n(\mathbf{S}) = 0$	$n(\mathbf{S}) = 1$

Since one must have $n(\mathbf{S}) - n(\mathbf{D}) \in \{0, 2\}$, as the nonzero eigenvalues for Eq. (5.5) are purely imaginary, one can conclude that

$$k_i^- = \begin{cases} 1, & a = -1 \\ 0, & a = +1 \end{cases}, \quad k_i^+ = 1 - k_i^-.$$

Now consider the radially symmetric vortex solution given in Eq. (3.16). One eventually sees that for Eq. (5.5),

$$\mathbf{S}_+ = -g_\ell\pi a y_1^2 \operatorname{diag} (4g_2 - 1, 3/2, 1/2), \quad \mathbf{S}_- = -g_\ell\pi a y_1^2 \operatorname{diag} (4g_2 - 1, 1/2, 3/2)$$

$$\mathbf{S}_2 = -\frac{1}{2}g_\ell\pi a y_1^2 \begin{pmatrix} 0 & 0 & 0 \\ 0 & 0 & 1 \\ 0 & 1 & 0 \end{pmatrix}.$$

One sees that for Eq. (5.5) the subspace $\operatorname{Span}(\{\mathbf{e}_1, \mathbf{e}_4\})$ is invariant; furthermore, the eigenvalue associated with this subspace is

$$\lambda_1^2 = -[g_\ell\pi a y_1^2(4g_2 - 1)]^2. \quad (5.22)$$

Upon reordering the remaining basis vectors via the mapping

$$\{\mathbf{e}_2, \mathbf{e}_3, \mathbf{e}_5, \mathbf{e}_6\} \mapsto \{\mathbf{e}_2, \mathbf{e}_6, \mathbf{e}_3, \mathbf{e}_5\}, \quad (5.23)$$

one sees that the remaining eigenvalues for Eq. (5.5) can be found via solving $\mathbf{AB}\mathbf{x} = \lambda_1^2\mathbf{x}$, where

$$\mathbf{A} := -\frac{1}{2}g_\ell\pi a y_1^2 \begin{pmatrix} 1 & 1 \\ -1 & -1 \end{pmatrix}, \quad \mathbf{B} := -\frac{1}{2}g_\ell\pi a y_1^2 \begin{pmatrix} 1 & 3 \\ -3 & -1 \end{pmatrix}. \quad (5.24)$$

Now, the nonzero eigenvalue in the closed right half of the plane for Eq. (5.24) is given by

$$\lambda_1^2 = \operatorname{trace}(\mathbf{AB})$$

$$= -\frac{3}{2}(g_\ell\pi a y_1^2)^2. \quad (5.25)$$

Hence, the wave is spectrally stable. Arguing in a manner similar to that for the vortex ring one can further conclude that if $\ell' = 2, \dots, 6$ then

$$k_i^- = \begin{cases} 0, & a = -1 \\ 2, & a = +1 \end{cases}, \quad k_i^+ = 2 - k_i^-,$$

while $k_i^- = k_i^+ = 1$ for $\ell' \geq 7$.

6. Stability: Hamiltonian–Hopf bifurcations

In the previous sections the $\mathcal{O}(\epsilon)$ eigenvalues were determined. Herein we will locate the potentially unstable $\mathcal{O}(1)$ eigenvalues which arise from a Hamiltonian–Hopf bifurcation. This bifurcation is possible only if for the unperturbed problem there is the collision of eigenvalues of opposite sign, i.e., only for the eigenvalues $\lambda = \pm i4\ell/\ell'$, $\ell = 1, \dots, \ell'$. A preliminary theoretical result will be needed before the actual calculations are presented. The result is simply a generalization of that presented in [25, Appendix], and can be easily proved using the regular perturbation theory presented in, e.g., [30]. In particular, we first consider the collision of eigenvalues of opposite Krein sign in a nongeneric case which arises in applications.

6.1. Reduced eigenvalue problem: Theory

Consider a general form of Eq. (4.1), i.e.,

$$J\mathcal{L}u = \lambda u, \tag{6.1}$$

under the following scenario:

$$J := \begin{pmatrix} \mathbf{0} & \mathbb{1} \\ -\mathbb{1} & \mathbf{0} \end{pmatrix}, \quad \mathcal{L} = \mathcal{L}_0 + \epsilon\mathcal{L}_\epsilon,$$

with

$$\mathcal{L}_0 := \text{diag}(A_0, A_0), \quad \mathcal{L}_\epsilon := \begin{pmatrix} A_1 & B \\ B & A_2 \end{pmatrix}. \tag{6.2}$$

Here it is assumed that $0 < \epsilon \ll 1$, and that the operators A_j and B are self-adjoint on a Hilbert space X with inner product $\langle \cdot, \cdot \rangle$. Furthermore, it will again be assumed that the operators satisfy the assumptions given in [26, Section 2].

First suppose that $\epsilon = 0$. Let $\lambda^\pm \in n(\mathcal{L}) \cap \mathbb{R}^\pm$ each be semi-simple eigenvalues with multiplicity n_\pm ; furthermore, let the basis of each eigenspace be given by the orthonormal set $\{\psi_1^\pm, \dots, \psi_{n_\pm}^\pm\}$. When considering only those eigenvalues in the upper half of the complex plane, for Eq. (6.1) the eigenvalues and corresponding eigenfunctions are given by

$$\begin{aligned} \lambda &= -i\lambda^-: u_j^- = (\psi_j^-, -i\psi_j^-)^T, \quad j = 1, \dots, n_- \\ \lambda &= +i\lambda^+: u_j^+ = (\psi_j^+, i\psi_j^+)^T, \quad j = 1, \dots, n_+. \end{aligned} \tag{6.3}$$

If one assumes that $\lambda^- = -\lambda^+$, then there is a collision of eigenvalues with opposite Krein signature; in particular, n_- eigenvalues of negative sign have collided with n_+ eigenvalues of positive sign. Under this scenario the eigenspace associated with the colliding eigenvalues is also *semi-simple*. As discussed in [41], this is a codimension three phenomenon, and hence is nongeneric.

The location of the perturbed eigenvalues can be found in the following manner. First write the perturbed eigenvalue and eigenfunction using the expansion

$$\lambda = i\lambda^+ + \epsilon\lambda_1 + \mathcal{O}(\epsilon^2), \quad u = \sum_{j=1}^{n_-} c_j^- u_j^- + \sum_{j=1}^{n_+} c_j^+ u_j^+ + \mathcal{O}(\epsilon), \tag{6.4}$$

and set $\mathbf{c} := (c_1^-, \dots, c_{n_-}^-, c_1^+, \dots, c_{n_+}^+)^T \in \mathbb{C}^{n_-+n_+}$. Upon rewriting Eq. (6.1) as $\mathcal{L}u = \lambda J^{-1}u$ and using standard perturbation theory (e.g., see the proof of [26, Theorem 4.4]) one sees that the $\mathcal{O}(\epsilon)$ correction is found by solving the matrix system

$$\left[i2\lambda_1 \text{diag}(\mathbb{1}_-, -\mathbb{1}_+) - \begin{pmatrix} S_- & S_c \\ S_c^H & S_+ \end{pmatrix} \right] \mathbf{c} = \mathbf{0}, \tag{6.5}$$

where $(\cdot)^H$ stands for Hermitian conjugation and

$$(S_\pm)_{jk} = \langle (A_1 + A_2)\psi_j^\pm, \psi_k^\pm \rangle, \quad (S_c)_{jk} = \langle (A_1 - A_2)\psi_j^-, \psi_k^+ \rangle + i2\langle B\psi_j^-, \psi_k^+ \rangle. \tag{6.6}$$

In Eq. (6.5) one has that $\mathbb{1}_\pm \in \mathbb{R}^{n_\pm \times n_\pm}$ is the identity matrix; furthermore, $S_\pm \in \mathbb{R}^{n_\pm \times n_\pm}$ are symmetric.

Remark 6.1. Set

$$S := \begin{pmatrix} S_- & S_c \\ S_c^H & S_+ \end{pmatrix},$$

and note that S is Hermitian. Assume that $z(S) = 0$. Set $\gamma^2 := -i2\lambda$. Upon using the results presented in [26, Section 3], one then knows that with respect to the eigenvalue parameter γ for Eq. (6.5),

$$k_r + 2k_i^- + 2k_c = n(S) + n_+, \quad k_r \geq |n(S) - n_+|; \tag{6.7}$$

in other words,

$$k_i^- + k_c \leq \min\{n(S), n_+\}.$$

Since Eq. (6.5) is a finite-dimensional problem, one also has that

$$k_r + 2k_i^+ + 2k_c = p(S) + n_-, \quad k_r \geq |p(S) - n_-|; \tag{6.8}$$

in other words,

$$k_i^+ + k_c \leq \min\{p(S), n_-\}.$$

In conclusion, one has that

$$k_c \leq \min\{p(S), n(S), n_+, n_-\}, \quad k_r \geq |n(S) - n_+|. \tag{6.9}$$

Note that for Eq. (6.5) to have eigenvalues with nonzero real part one must have that $k_c \geq 1$. Thus, if S is positive definite, i.e., $n(S) = 0$, then as a consequence of Eqs. (6.7)–(6.9) one necessarily has that

$$k_r = n_+, \quad k_i^+ = n_-, \quad k_i^- = k_c = 0; \tag{6.10}$$

in other words, for Eq. (6.5) one has that $\lambda_1 \in i\mathbb{R}$ (also see [21, Corollary 1.1]).

6.2. Reduced eigenvalue problem: Real-valued solutions

Let us now apply the results of Section 6.1 to those solutions found in Section 3. Recall that from Section 3 the solutions bifurcate from $\lambda = 6$. Now, in general

$$\lambda_{m,\ell} < 6 \iff (m, \ell) \in \Sigma_n := \{(0, 0), (0, 1), \dots, (0, \ell' - 1)\},$$

whereas

$$\lambda_{m,\ell} > 6 \iff (m, \ell) \in \Sigma_p := (\mathbb{N}_0 \times \mathbb{N}_0) \setminus (\Sigma_n \cup \{(1, 0), (0, \ell')\}).$$

Furthermore, when $\epsilon = 0$ the eigenvalue $\lambda_{m,\ell}$ maps to $\pm i(6 - \lambda_{m,\ell})$. Thus, upon following the ideas presented in Section 6.1 one knows that a Hamiltonian–Hopf bifurcation will be associated with those eigenvalues which satisfy

$$6 - \lambda_{a,b} = \lambda_{c,d} - 6; \quad \lambda_{a,b} \in \Sigma_n, \quad \lambda_{c,d} \in \Sigma_p.$$

A simple calculation shows that the above is satisfied if

$$\begin{aligned} (a, b) = (0, 0): (c, d) &\in \{(0, 2\ell'), (1, \ell'), (2, 0)\} \\ (a, b) = (0, \ell): (c, d) &\in \{(0, 2\ell' - \ell), (1, \ell' - \ell)\}, \quad \ell = 1, \dots, \ell' - 1. \end{aligned} \tag{6.11}$$

As a consequence, in the upper half of the complex plane one has ℓ' distinct possible bifurcation points. Furthermore, if $(a, b) = (0, 0)$, then $n_- = 1$; otherwise, $n_- = 2$. In both cases, the geometric multiplicity of the semi-simple eigenvalue is six.

First consider the real-valued solutions. Upon using Eq. (3.3), set

$$Q := x_1 q_{1,0}(r) + y_1 q_{0,\ell'}(r) \cos \ell' \theta. \tag{6.12}$$

In Eq. (6.2) one then has that

$$A_1 = -(\Delta\omega + 3aQ^2), \quad A_2 = -(\Delta\omega + aQ^2), \quad B = 0, \tag{6.13}$$

where the result of Eq. (6.12) must be appropriately substituted.

First suppose that $(a, b) = (0, 0)$, so that $n_- = 1$ and $n_+ = 5$. In this case set

$$\begin{aligned} \psi_1^- &= q_{0,0}(r), & \psi_1^+ &= q_{0,2\ell'}(r) \cos 2\ell'\theta, \\ \psi_2^+ &= q_{0,2\ell'}(r) \sin 2\ell'\theta, & \psi_3^+ &= q_{1,\ell'}(r) \cos \ell'\theta, \\ \psi_4^+ &= q_{1,\ell'}(r) \sin \ell'\theta, & \psi_5^+ &= q_{2,0}(r). \end{aligned} \tag{6.14}$$

Upon using Eqs. (6.13) and (6.14) in Eq. (6.6), as well as some standard trigonometric identities, one sees that the only nonzero off-diagonal entries for S_+ (recall that it is symmetric) are given by

$$\begin{aligned} y_1 = 0: & \text{none} \\ x_1 = 0: & (S_+)_{15} \\ x_1 y_1 \neq 0: & (S_+)_{15}, (S_+)_{35}. \end{aligned} \tag{6.15}$$

Regarding the matrix S_c one has that the only possible nonzero entries are given by

$$\begin{aligned} y_1 = 0: & (S_c)_{15} \\ x_1 = 0: & (S_c)_{11}, (S_c)_{15} \\ x_1 y_1 \neq 0: & (S_c)_{11}, (S_c)_{13}, (S_c)_{15}. \end{aligned} \tag{6.16}$$

In conclusion, one has in each case that a Hamiltonian–Hopf bifurcation can occur only through the following mode interactions:

Solution	$K < 0$	$K > 0$
<i>ring</i>	ψ_1^-	ψ_5^+
<i>multi-pole</i>	ψ_1^-	ψ_1^+, ψ_5^+
<i>soliton necklace</i>	ψ_1^-	$\psi_1^+, \psi_3^+, \psi_5^+$

(6.17)

In Eq. (6.17) the parameter K refers to the sign of the eigenvalue corresponding to that eigenfunction.

Now suppose that $(a, b) = (0, \ell)$, so that $n_- = 2$ and $n_+ = 4$. In this case set

$$\begin{aligned} \psi_1^- &= q_{0,\ell}(r) \cos \ell\theta, & \psi_2^- &= q_{0,\ell}(r) \sin \ell\theta, \\ \psi_1^+ &= q_{0,2\ell'-\ell}(r) \cos(2\ell' - \ell)\theta, & \psi_2^+ &= q_{0,2\ell'-\ell}(r) \sin(2\ell' - \ell)\theta, \\ \psi_3^+ &= q_{1,\ell'-\ell}(r) \cos(\ell' - \ell)\theta, & \psi_4^+ &= q_{1,\ell'-\ell}(r) \sin(\ell' - \ell)\theta. \end{aligned} \tag{6.18}$$

Upon using Eqs. (6.13) and (6.18) in Eq. (6.6), as well as some standard trigonometric identities, one sees that the only nonzero off-diagonal entries for S_+ (recall that it is symmetric) are given by

$$\begin{aligned} x_1 y_1 = 0: & \text{none} \\ x_1 y_1 \neq 0: & (S_+)_{13}, (S_+)_{24}. \end{aligned} \tag{6.19}$$

Regarding the matrix S_c there are two cases to consider. First suppose that $2\ell \neq \ell'$. One then has that

$$\begin{aligned} y_1 = 0: & \text{none} \\ x_1 = 0: & (S_c)_{11}, (S_c)_{22} \\ x_1 y_1 \neq 0: & (S_c)_{11}, (S_c)_{22}, (S_c)_{13}, (S_c)_{24}. \end{aligned} \tag{6.20}$$

If $2\ell = \ell'$, then one has that the only possible nonzero entries are given by

$$\begin{aligned} y_1 = 0: & (S_c)_{13}, (S_c)_{24} \\ x_1 = 0: & (S_c)_{11}, (S_c)_{22} \\ x_1 y_1 \neq 0: & (S_c)_{11}, (S_c)_{22}, (S_c)_{13}, (S_c)_{24}. \end{aligned} \tag{6.21}$$

Finally, in all cases S_- is diagonal. In conclusion, one has in each case that a Hamiltonian–Hopf bifurcation can occur only through the following mode interactions. First, if $2\ell \neq \ell'$, then one has that:

Solution	$K < 0$	$K > 0$
ring	ψ_1^-	none
	ψ_2^-	none
multi-pole	ψ_1^-	ψ_1^+
	ψ_2^-	ψ_2^+
soliton necklace	ψ_1^-	ψ_1^+, ψ_3^+
	ψ_2^-	ψ_2^+, ψ_4^+

(6.22)

On the other hand, if $2\ell = \ell'$, then one has that:

Solution	$K < 0$	$K > 0$
ring	ψ_1^-	ψ_3^+
	ψ_2^-	ψ_4^+
multi-pole	ψ_1^-	ψ_1^+
	ψ_2^-	ψ_2^+
soliton necklace	ψ_1^-	ψ_1^+, ψ_3^+
	ψ_2^-	ψ_2^+, ψ_4^+

(6.23)

Let us now illustrate the above calculations with a couple of examples. The relevant eigenfunctions in Eqs. (6.14) and (6.18) which are needed to explicitly compute the above quantities are given by

$$\begin{aligned}
 q_{0,0}(r) &= \sqrt{\frac{1}{\pi}} e^{-r^2/2}, & q_{1,0}(r) &= \sqrt{\frac{1}{\pi}} (1 - r^2)e^{-r^2/2}, & q_{2,0}(r) &= \sqrt{\frac{1}{4\pi}} (2 - 4r^2 + r^4)e^{-r^2/2} \\
 q_{0,\ell}(r) &= \sqrt{\frac{2}{\ell!\pi}} r^\ell e^{-r^2/2}, & q_{1,\ell}(r) &= \sqrt{\frac{2}{(\ell+1)!\pi}} ((\ell+1) - r^2)r^\ell e^{-r^2/2}.
 \end{aligned}$$
(6.24)

6.2.1. Example: Ring

First consider the ring solution, i.e., suppose that $y_1 = 0$ in Eq. (6.12). For $\lambda = i4 + \mathcal{O}(\epsilon)$, use of the theory presented in Section 6.1 and the result of Eq. (6.17) yields that the only nontrivial interaction is that of $\psi_1^- = q_{0,0}$ with $\psi_5^+ = q_{2,0}$ (see Eq. (6.14)). By Eq. (6.5) the relevant eigenvalue problem is given by

$$\left[i2\lambda_1 \begin{pmatrix} 1 & 0 \\ 0 & -1 \end{pmatrix} - \begin{pmatrix} \langle (A_1 + A_2)\psi_1^-, \psi_1^- \rangle & \langle (A_1 - A_2)\psi_5^+, \psi_1^- \rangle \\ \langle (A_1 - A_2)\psi_5^+, \psi_1^- \rangle & \langle (A_1 + A_2)\psi_5^+, \psi_5^+ \rangle \end{pmatrix} \right] \mathbf{c} = \mathbf{0}.$$
(6.25)

Upon using Eqs. (3.9), (6.13) and (6.24), one eventually sees that the eigenvalues for Eq. (6.25) are given by

$$\lambda_1 = -i\frac{1}{8}\Delta\omega, \quad \lambda_1 = -i\frac{1}{4}\Delta\omega.$$
(6.26)

Thus, by Eq. (6.4) one has that no Hamiltonian–Hopf bifurcation occurs at this point.

Now suppose that $\lambda = i4(1 - \ell/\ell') + \mathcal{O}(\epsilon)$, $\ell = 1, \dots, \ell' - 1$. If $2\ell \neq \ell'$, then by Eq. (6.22) one can immediately conclude that there is no Hamiltonian–Hopf bifurcation. Now suppose that $2\ell = \ell'$. Use of the theory presented in Section 6.1 and the result of Eq. (6.23) yields that there are two relevant eigenvalue problems. Since the solution is radially symmetric, each problem will yield the same answer; hence, it is enough to focus on the $\{\psi_1^-, \psi_3^+\}$ -interaction (see Eq. (6.18)). Proceeding in a manner similar to that which leads to Eq. (6.25) gives the relevant eigenvalue problem to be

$$\left[i2\lambda_1 \begin{pmatrix} 1 & 0 \\ 0 & -1 \end{pmatrix} - \begin{pmatrix} \langle (A_1 + A_2)\psi_1^-, \psi_1^- \rangle & \langle (A_1 - A_2)\psi_3^+, \psi_1^- \rangle \\ \langle (A_1 - A_2)\psi_3^+, \psi_1^- \rangle & \langle (A_1 + A_2)\psi_3^+, \psi_3^+ \rangle \end{pmatrix} \right] \mathbf{c} = \mathbf{0},$$

i.e.,

$$(\lambda_1 \text{diag}(1, -1) - i\Delta\omega \mathbf{S}) \mathbf{c} = \mathbf{0},$$
(6.27)

where

$$S_{11} = 1 - \frac{\ell^2 - \ell + 2}{2^\ell}, \quad S_{12} = -\frac{(\ell^2 - 3\ell + 2)\sqrt{\ell + 1}}{2^{\ell+2}}, \quad S_{22} = 1 - \frac{\ell^3 - 3\ell^2 + 2\ell - 8}{2^{\ell+2}}.$$

Since $n(\mathbf{S}) = 0$ for $\ell \geq 4$, by Eq. (6.10) one has that a Hamiltonian–Hopf bifurcation cannot occur for $\ell \geq 4$. A numerical examination of Eq. (6.27) for $\ell = 2, 3$ reveals that $\lambda_1 \in i\mathbb{R}$ for these values also. Consequently, there is never a Hamiltonian–Hopf bifurcation associated with these eigenvalues.

Lemma 6.2. *When considering the ring solution, there are no Hamiltonian–Hopf bifurcations associated with the eigenvalues*

$$\lambda = i4 \frac{\ell}{\ell'}, \quad \ell = 1, \dots, \ell'.$$

Remark 6.3. Combining the results of Eq. (5.2) with the above analysis reveals that the ring solution is spectrally stable for $\ell' \geq 6$.

6.2.2. Example: Multi-pole

Consider now the multi-pole solution, i.e., suppose that $x_1 = 0$ in Eq. (6.12). For $\lambda = i4 + \mathcal{O}(\epsilon)$, use of the theory presented in Section 6.1 and the result of Eq. (6.17) yields that the relevant interaction is that of $\psi_1^- = q_{0,0}$ with $\psi_1^+ = q_{0,2\ell'}(r) \cos 2\ell'\theta$ and $\psi_5^+ = q_{2,0}$ (see Eq. (6.14)). Hence, in this case one must solve a 3×3 eigenvalue problem, which after some simplification is given by

$$(\lambda_1 \text{diag}(1, -1, -1) - i\Delta\omega \mathbf{S})\mathbf{c} = \mathbf{0}, \tag{6.28}$$

where

$$\begin{aligned} S_{11} &= 1 - \frac{4}{3} \frac{2^{\ell'} (\ell')^2}{(2\ell')!}, & S_{12} &= -\frac{\sqrt{2}}{3} \frac{\ell'!}{\sqrt{(2\ell')!}}, \\ S_{13} &= -\frac{1}{12} \frac{2^{\ell'} (\ell')^2}{(2\ell')!} (\ell'^2 - 5\ell' + 2), & S_{22} &= 1 - \frac{4}{3} \frac{2^{-\ell'} \ell'! (3\ell')!}{[(2\ell')!]^2}, \\ S_{23} &= -\frac{\sqrt{2}}{6} \frac{\ell'!}{\sqrt{(2\ell')!}} (2\ell'^2 - 5\ell' + 4), & S_{33} &= 1 - \frac{1}{48} \frac{2^{\ell'} (\ell')^2}{(2\ell')!} (\ell'^4 - 6\ell'^3 + 19\ell'^2 - 14\ell' + 24). \end{aligned}$$

An application of Stirling’s formula shows that $\mathbf{S} \rightarrow \mathbb{1}$ as $\ell' \rightarrow \infty$; hence, by Eq. (6.10) one has that a Hamiltonian–Hopf bifurcation cannot occur for ℓ' sufficiently large. A numerical examination of Eq. (6.28) shows that a Hamiltonian–Hopf bifurcation indeed occurs for $\ell' = 2$, but that no such bifurcation occurs for any $\ell' \geq 3$.

Now suppose that $\lambda = i4(1 - \ell/\ell') + \mathcal{O}(\epsilon)$, $\ell = 1, \dots, \ell' - 1$. Use of the theory presented in Section 6.1 and the result of Eq. (6.23) yields that there are two relevant eigenvalue problems: the $\{\psi_1^-, \psi_1^+\}$ -interaction and the $\{\psi_2^-, \psi_2^+\}$ -interaction (again see Eq. (6.18)). First consider the $\{\psi_1^-, \psi_1^+\}$ -interaction. Proceeding in a manner similar to that which leads to Eq. (6.25) eventually yields the reduced eigenvalue problem

$$(\lambda_1 \text{diag}(1, -1) - i\Delta\omega \mathbf{S})\mathbf{c} = \mathbf{0}, \tag{6.29}$$

where

$$S_{11} = 1 - \frac{4}{3} \frac{2^{\ell'-\ell} \ell'! (\ell' + \ell)!}{\ell! (2\ell')!}, \quad S_{12} = \frac{1}{3} \sqrt{\frac{(\ell')^2}{\ell! (2\ell' - \ell)!}}, \quad S_{22} = 1 - \frac{4}{3} \frac{2^{-(\ell'-\ell)} \ell'! (3\ell' - \ell)!}{(2\ell')! (2\ell' - \ell)!}.$$

Remark 6.4. If one considers the $\{\psi_2^-, \psi_2^+\}$ -interaction, then all that changes in Eq. (6.29) is that $S_{12} \mapsto -S_{12}$. This does not change any of the analysis, nor any of the subsequent conclusions.

The eigenvalues for Eq. (6.29) are given by

$$\lambda_1 = \frac{1}{2} \left(S_{11} - S_{22} \pm \sqrt{(S_{11} + S_{22})^2 - 4S_{12}^2} \right). \tag{6.30}$$

If one sets

$$H(\mathbf{S}) := (S_{11} + S_{22})^2 - 4S_{12}^2,$$

then one has that $H(\mathbf{S}) = 0$ defines a Hamiltonian–Hopf bifurcation threshold. In particular, if $H(\mathbf{S}) < 0$, then such a bifurcation will occur, whereas if $H(\mathbf{S}) > 0$ there will be no bifurcation.

First suppose that $\ell = \ell' - 1$. One then has that

$$\lambda_1 = \left(\frac{\pm \sqrt{\ell'^2 + \ell' - 1} - i\ell'}{3(\ell' + 1)} \right) \Delta\omega;$$

in other words, there is a Hamiltonian–Hopf bifurcation for all $\ell' \geq 2$. Now suppose that $\ell = \ell' - k$ for some fixed $k \geq 2$. For $k^2/\ell' \ll 1$ one has the asymptotics

$$S_{11} \sim -\frac{1}{3} + \frac{2}{3} \frac{k(k-1)}{\ell'}, \quad S_{22} \sim -\frac{1}{3} + \frac{1}{3} \frac{k(k+1)}{\ell'}, \quad S_{12}^2 \sim \frac{1}{9} \left(1 - \frac{k^2}{\ell'}\right),$$

so that

$$H(S) \sim -\frac{4}{9} \frac{k(2k-1)}{\ell'} \in \mathbb{R}^-, \quad \frac{k^2}{\ell'} \ll 1.$$

Consequently, for each fixed value of k there is a value ℓ'_m such that a Hamiltonian–Hopf bifurcation occurs for $\ell' \geq \ell'_m$. A table of such values is given in Eq. (6.31). No Hamiltonian–Hopf bifurcation occurs for the fixed value of k if $\ell' < \ell'_m$.

k	1	2	3	4	5	6	7	8	9	10	11	12	13	14	15
ℓ'_m	2	3	5	9	15	21	28	37	47	57	69	83	97	112	129

(6.31)

Finally, if ℓ is fixed independent of ℓ' , then an application of Stirling’s formula shows that $S \rightarrow 1$ as $\ell' \rightarrow \infty$; hence, by Eq. (6.10) one has that a Hamiltonian–Hopf bifurcation cannot occur for that value of ℓ for ℓ' sufficiently large.

Lemma 6.5. *When considering the multi-pole solution, for each $2 \leq k \leq \ell' - 1$ there is a Hamiltonian–Hopf bifurcation from the eigenvalue $\lambda = ik/\ell'$ for $\ell' \geq \ell'_m$, where numerically computed values of ℓ'_m are given in Eq. (6.31). Two eigenvalues emerge into the open right half of the complex plane from these points; furthermore, to leading order these eigenvalues are semi-simple. Finally, if $\ell' = 2$, then there is a Hamiltonian–Hopf bifurcation associated with the eigenvalue $\lambda = i4$.*

Remark 6.6. Unlike the ring solution, the multi-pole solution is never spectrally stable. Recalling Remark 6.4, one has that if $\ell' = 2$, then there are three eigenvalues in the open first quadrant of the complex plane; otherwise, there is an even number of eigenvalues in the open first quadrant of the complex plane. Furthermore, as ℓ' increases the number of unstable eigenvalues monotonically increases.

6.3. Reduced eigenvalue problem: Complex-valued solutions

Now consider the complex-valued solutions; in particular, those given in Eqs. (3.14) and (3.16). Write

$$Q := U + iV, \tag{6.32}$$

where the particular form of U and V can be deduced from Lemma 3.3. In Eq. (6.2) one then has that

$$A_1 = -\Delta\omega - a(3U^2 + V^2), \quad A_2 = -\Delta\omega - a(U^2 + 3V^2), \quad B = -2aUV, \tag{6.33}$$

where the result of Eq. (6.32) must be appropriately substituted. Proceeding as above, one can generate the following tables. The analogue to Eq. (6.17) is given by

Solution	$K < 0$	$K > 0$
<i>vortex</i>	ψ_1^-	ψ_1^+, ψ_2^+
<i>vortex necklace</i>	ψ_1^-	$\psi_1^+, \psi_4^+, \psi_5^+$

(6.34)

Here *vortex* refers to the radially symmetric solution given in Eq. (3.16), while the *vortex necklace* refers to that given in Eq. (3.14). For $2\ell \neq \ell'$, the analogue to Eq. (6.22) is given by

Solution	$K < 0$	$K > 0$
<i>vortex</i>	ψ_1^-, ψ_2^-	ψ_1^+, ψ_2^+
<i>vortex necklace</i>	ψ_1^- ψ_2^-	ψ_1^+, ψ_4^+ ψ_2^+, ψ_3^+

(6.35)

whereas if $2\ell = \ell'$, then the analogue to Eq. (6.23) is given by

Solution	$K < 0$	$K > 0$
<i>vortex</i>	ψ_1^-, ψ_2^-	ψ_1^+, ψ_2^+
<i>vortex necklace</i>	ψ_1^-, ψ_2^-	$\psi_1^+, \psi_2^+, \psi_3^+, \psi_4^+$

(6.36)

6.3.1. Example: Vortex

Consider the vortex solution, i.e., suppose that $x_1 = 0$. For $\lambda = i4 + \mathcal{O}(\epsilon)$, use of the theory presented in Section 6.1 and the result of Eq. (6.34) yields that the relevant interaction is that of $\psi_1^- = q_{0,0}$ with $\psi_1^+ = q_{0,2\ell'}(r) \cos 2\ell'\theta$ and $\psi_2^+ = q_{0,2\ell'}(r) \sin 2\ell'\theta$ (see Eq. (6.14)). Hence, in this case one must solve a 3×3 eigenvalue problem, which after some simplification is given by

$$(\lambda_1 \text{diag}(1, -1, -1) - i\Delta\omega\mathbf{S})\mathbf{c} = \mathbf{0}, \tag{6.37}$$

where using the notation presented in Eq. (6.5) one has that

$$\mathbf{S}_- = S_-(1), \quad \mathbf{S}_+ = S_+ \text{diag}(1, 1), \quad \mathbf{S}_c = S_c(1, i).$$

with

$$S_- = 1 - 2^{1+\ell'} \frac{(\ell')^2}{(2\ell')!}, \quad S_+ = 1 - 2^{1-\ell'} \frac{\ell'!(3\ell')!}{[(2\ell')!]^2}, \quad S_c = -\frac{\sqrt{2}}{2} \frac{\ell'!}{\sqrt{(2\ell')!}}.$$

The eigenvalues for Eq. (6.37) are given by

$$\lambda_1 = -S_+, \frac{S_- - S_+ \pm \sqrt{(S_- + S_+)^2 - 8S_c^2}}{2}.$$

An application of Stirling’s formula shows that $(S_- + S_+)^2 - 8S_c^2 \in \mathbb{R}^+$ for $\ell' \gg 1$; hence, a Hamiltonian–Hopf bifurcation cannot occur for ℓ' sufficiently large. A numerical examination shows that a Hamiltonian–Hopf bifurcation occurs only for $\ell' = 2, 3$, but that no such bifurcation occurs for any $\ell' \geq 4$.

Now suppose that $\lambda = i4(1 - \ell/\ell') + \mathcal{O}(\epsilon)$, $\ell = 1, \dots, \ell' - 1$. Use of the theory presented in Section 6.1 and the result of Eqs. (6.35) and (6.36) yields that the relevant eigenvalue problem is the $\{\psi_1^-, \psi_2^-, \psi_1^+, \psi_2^+\}$ -interaction (see Eq. (6.18)). Again using the notation presented in Eq. (6.5) one eventually obtains the reduced eigenvalue problem

$$(\lambda_1 \text{diag}(1, 1, -1, -1) - i\Delta\omega\mathbf{S})\mathbf{c} = \mathbf{0}, \tag{6.38}$$

where

$$\mathbf{S}_- = S_- \text{diag}(1, 1), \quad \mathbf{S}_+ = S_+ \text{diag}(1, 1), \quad \mathbf{S}_c = S_c \begin{pmatrix} 1 & i \\ i & -1 \end{pmatrix},$$

with

$$S_- = 1 - 2^{\ell'-\ell+1} \frac{\ell'!(\ell'+\ell)!}{\ell!(2\ell')!}, \quad S_+ = 1 - 2^{-(\ell'-\ell-1)} \frac{\ell'!(3\ell'-\ell)!}{(2\ell'-\ell)!(2\ell')!}, \quad S_c = -\frac{1}{2} \frac{\ell'!}{\sqrt{\ell!(2\ell'-\ell)!}}.$$

The eigenvalues for Eq. (6.38) are given by

$$\lambda_1 = S_-, -S_+, \frac{S_- - S_+ \pm \sqrt{(S_- + S_+)^2 - 16S_c^2}}{2}, \tag{6.39}$$

hence, out of each point at most one eigenvalue can enter the open right half of the complex plane. If one sets

$$H(\mathbf{S}) := (S_- + S_+)^2 - 16S_c^2, \tag{6.40}$$

then one has that $H(\mathbf{S}) = 0$ defines a Hamiltonian–Hopf bifurcation threshold. In particular, if $H(\mathbf{S}) < 0$, then such a bifurcation takes place, whereas if $H(\mathbf{S}) > 0$ there will be no bifurcation.

First suppose that $\ell = \ell' - 1$. The eigenvalues of Eq. (6.39) then become

$$\lambda_1 = -1, -\frac{1}{\ell'+1}, 0, \frac{\ell'}{\ell'+1},$$

so that no Hamiltonian–Hopf bifurcation occurs at this point. Now suppose that $\ell = \ell' - k$ for some fixed $k \geq 2$. For $k^2/\ell' \ll 1$ one has the asymptotics

$$S_- \sim -1 + \frac{k(k-1)}{\ell'}, \quad S_+ \sim -1 + \frac{1}{2} \frac{k(k+1)}{\ell'}, \quad S_c^2 \sim \frac{1}{4} \left(1 - \frac{k^2}{\ell'}\right),$$

so that

$$H(\mathbf{S}) \sim -2 \frac{k(k-1)}{\ell'} \in \mathbb{R}^-, \quad \frac{k^2}{\ell'} \ll 1.$$

Consequently, for each fixed value of k there is a value ℓ'_v such that a Hamiltonian–Hopf bifurcation occurs for $\ell' \geq \ell'_v$. A table of such values is given in Eq. (6.41). No Hamiltonian–Hopf bifurcation occurs for the fixed value of k if $\ell' < \ell'_v$.

k	1	2	3	4	5	6	7	8	9	10	11	12	13	14	15
ℓ'_v	∞	3	4	5	8	11	15	19	24	29	35	42	49	56	64

(6.41)

Finally, if ℓ is fixed independent of ℓ' , then an application of Stirling’s formula shows that $S \rightarrow \mathbb{1}$ as $\ell' \rightarrow \infty$; hence, by Eq. (6.10) one has that a Hamiltonian–Hopf bifurcation cannot occur for that value of ℓ for ℓ' sufficiently large.

Lemma 6.7. *When considering the vortex solution, for each $2 \leq k \leq \ell' - 1$ there is a Hamiltonian–Hopf bifurcation from the eigenvalue $\lambda = i4k/\ell'$ for $\ell' \geq \ell'_v$, where numerically computed values of ℓ'_v are given in Eq. (6.41). One eigenvalue emerges into the open right half of the complex plane from these points. Furthermore, if $\ell' = 2, 3$, then there is a Hamiltonian–Hopf bifurcation associated with the eigenvalue $\lambda = i4$.*

Remark 6.8. As is also true for the multi-pole solution, the vortex solution for $\ell' \geq 2$ is never spectrally stable. Furthermore, as ℓ' increases the number of unstable eigenvalues monotonically increases.

Remark 6.9. It should be noted that numerical calculations relating to Eqs. (6.34) and (6.36) in the case of the vortex with $\ell' = 2$ are given in [36, Section 7.3]. Therein it is seen that the $\{\psi_1^-, \psi_1^+, \psi_2^+\}$ -interaction given in Eq. (6.34) leads to a Hamiltonian–Hopf bifurcation, whereas the interaction detailed in Eq. (6.36) does not.

Remark 6.10. For $\ell' = 4$, i.e., for $\Omega = \Omega_4 = -1$, one has as a consequence of Lemma 6.7 that a Hamiltonian–Hopf bifurcation arises from a $\{q_{0,2}e^{\pm i2\theta}, q_{0,6}e^{\pm i6\theta}\}$ -interaction ($\lambda = i2$) and a $\{q_{0,1}e^{\pm i\theta}, q_{0,7}e^{\pm i7\theta}\}$ -interaction ($\lambda = i3$). In [31] it is shown numerically that for the case $\ell' = 4$ with $\Omega = 0$ the Hamiltonian–Hopf bifurcations result from a $\{q_{0,2}e^{\pm i2\theta}, q_{2,2}e^{\pm i2\theta}\}$ -interaction and a $\{q_{0,3}e^{\pm i3\theta}, q_{1,3}e^{\pm i3\theta}\}$ -interaction. The difference is due to the fact that in a rotating frame the spectrum is shifted vertically, which leads to different eigenvalue collisions. Thus, in a rotating coordinate frame the type of interactions which lead to an instability is changed, even though the underlying solution does not depend upon the rotation frequency. The interested reader should also compare the results of Lemma 6.7 with those of [49] for the case of $\ell' = 3$.

Remark 6.11. If for the perturbed problem one writes

$$\begin{aligned} \lambda_{0,\ell} &= 2 + 4\ell + \ell\Omega_{\ell'} + \Delta\lambda_{0,\ell}\epsilon + \mathcal{O}(\epsilon^2) \\ \lambda_{0,2\ell'-\ell} &= 2 + 4(2\ell' - \ell) + (2\ell' - \ell)\Omega_{\ell'} + \Delta\lambda_{0,2\ell'-\ell}\epsilon + \mathcal{O}(\epsilon^2), \end{aligned}$$

then it is not difficult to show that the threshold condition $H(S) < 0$ can to leading order be rewritten as

$$|\Delta\lambda_{0,\ell} + \Delta\lambda_{0,2\ell'-\ell}| < \frac{2}{g_{\ell'}} \langle q_{0,\ell'}^2, q_{0,\ell}q_{0,2\ell'-\ell} \rangle |\Delta\omega|.$$

A similar threshold condition is given in [49, Eq. (6)]. However, unlike the results presented herein, the upper bound in [49] was computed numerically.

7. Numerical results

We now proceed to numerically examine the relevant solutions established in the previous sections. Our numerical results will corroborate the theoretically obtained picture for the case of $\ell' = 2$ ($\Omega_{\ell'} = 0$). We will examine the focusing case of attractive interactions ($a = +1$), in particular, in what follows for illustration purposes. It should be noted, however, that in the previous sections relevant changes for the defocusing case of repulsive interactions have been discussed. In fact, the only possible difference between the two cases is the Krein signature of the $\mathcal{O}(\epsilon)$ nonzero eigenvalues. We use a fixed point Newton algorithm [6] to numerically identify the solutions up to a prescribed tolerance (typically 10^{-7} – 10^{-8}). As a starting guess for the fixed point iteration, we use our theoretical approximation of Sections 3.2 and 3.3 and typically find this approximation to converge to the (numerically) exact solution within a few iteration steps. Once the algorithm converges, numerical linear stability is performed on the corresponding branches to obtain the relevant eigenvalues of the linearization spectrum. This is done using a standard numerical linear algebra (LAPACK) eigenvalue solver. For unstable solutions, we also use appropriately crafted “numerical experiments” to showcase the dynamical evolution associated with the instability. In these we initialize the dynamics with the relevant unstable configuration, perturbed by a small amplitude (typically 10^{-4}) multiplying an instability eigenvector of the linearization. This accelerates the manifestation of the respective instabilities, facilitating their observation in our evolution simulations. The time integration is performed using a standard fourth-order Runge–Kutta algorithm [6].

Fig. 3 shows our results for the ring-like real-valued solution (namely, the first one among the ones of Eq. (3.9)). For this solution, as predicted by the results tabulated in Eq. (5.2), we find two real eigenvalue pairs contributing to the instability of the relevant mode.

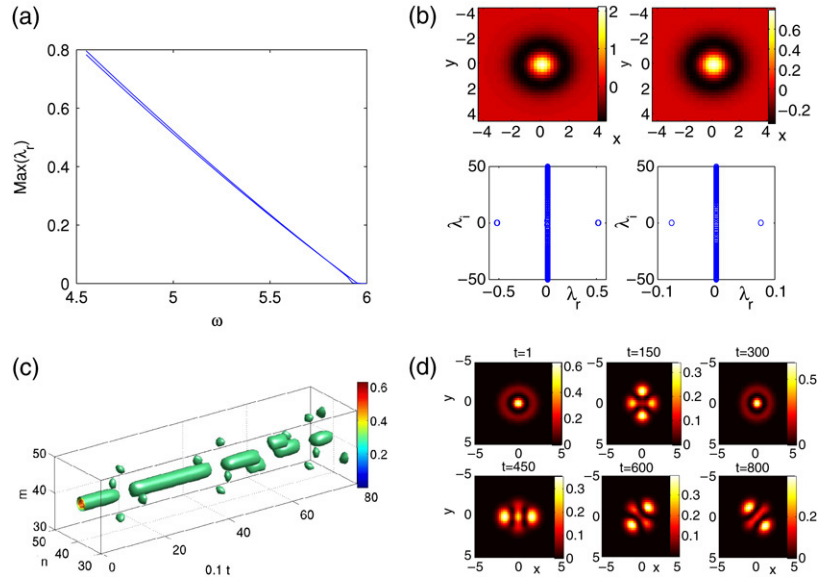


Fig. 3. (Color online) The figure shows the bifurcation analysis (top panels) and dynamical evolution (bottom panels) of the simplest real solution, namely the ring structure. Panel (a) illustrates the dependence on the chemical potential ω of the two real eigenvalues (with approximately equal magnitudes) that we find this configuration to possess. Panel (b) shows two typical examples of the structure (top) and of the spectral plane of its linearization (bottom) for the cases with $\omega = 5$ (left panels) and that with $\omega = 5.8$ (right panels, closer to the linear limit). Panel (c) shows in a 3d graph the space-time evolution of the ring-like condensate. The spatial variables $m = 40 + x/h$ and $n = 40 + y/h$, where h is the numerically used grid spacing of $h = 0.23$. The evolution runs until $t = 800$ and is commented in detail in the text. Panel (d) facilitates the reading of panel (c) by offering two-dimensional cross-sections (along the time axis) illustrating the configuration profile at appropriately selected times during the evolution.

These eigenvalues are nearly identical as is shown in panel (a) of the figure which agrees with the theoretical prediction discussed around Eq. (5.13). Panel (b) of the figure illustrates the configuration (top) and the spectral plane of the imaginary (λ_i) versus the real (λ_r) part of the eigenvalues λ for the cases of $\omega = 5.8$ (right; close to the linear limit) and $\omega = 5$ (left; further away from that limit). Since the configuration is unstable in the two bottom panels, we have examined its instability through a relevant numerical experiment (for the case with $\omega = 5.8$), as outlined above. Panel (c) encompasses the spatio-temporal (x , y and t) evolution of the solution's contour up to $t = 800$. Details of the relevant evolution are given in panel (d) which contains specific snapshots (at $t = 1, 150, 300, 450, 600$ and 800) of the spatial profile. It can clearly be seen that around $t \approx 150$, the solution breaks up into a quadrupolar structure as a result of the instability; this is also natural to expect based on the relevant instability eigenvector from our earlier stability analysis. The circular structure recurs (see e.g., the snapshot at $t = 300$ in panel (d) and also the relevant re-appearance of the initial structure in panel (c)). Later, however, (for $t > 400$), the quadrupolar structure re-emerges, as well as more complicated structures (as shown in the last 3 plots of panel (d)), interrupted by shorter recurrences of the original state.

We now turn to the second real-valued solution of Eq. (3.9), namely the multi-pole (quadrupole for $\ell' = 2$) structure that is illustrated in Fig. 4. For this solution, panel (a) confirms the theoretical stability prediction of Lemma 6.5 and the ensuing remark, in that we find four eigenvalues with nonvanishing real parts in the first quadrant of the spectral plane. We confirm that one of them is real in accordance with the discussion around Eq. (5.15), while three of them stem from Hamiltonian–Hopf bifurcations, as is more clearly shown in panel (b). In fact, zooming into the relevant spectral plane pictures (especially the right ones of $\omega = 5.8$) identifies one of the pairs as stemming from such a bifurcation occurring at $\lambda = \pm i4$, while the other two pairs emerge from $\lambda = \pm i2$ (see Lemma 6.5). Panels (c) and (d), as before, showcase the dynamical evolution of the pertinent instability for the case of $\omega = 5.8$ through a spatio-temporal contour evolution as well as through snapshots at different times. Both of these indicate that around $t \approx 150$, the configuration distorts itself towards a structure with 3 peaks (in fact, somewhat resembling our third real-valued, soliton necklace solution), but then returns to its original profile, only to be further, and more dramatically, distorted at later times, especially above $t = 300$.

Next, we consider the last real-valued solution, i.e., the soliton necklace of Eq. (3.10). In this case the results are shown in Fig. 5. Panel (a) indicates that in this case there is no real eigenvalue, in accordance with Eq. (5.2). However, there is a complex eigenvalue quartet in both panels (a) and (b), which can be observed (upon appropriate zoom into panel (b)) to bifurcate from $\lambda = \pm i4$ in this case. Panels (c) and (d) show the evolution of the corresponding Hamiltonian–Hopf bifurcation for the configuration when $\omega = 5.375$. It is worthwhile to pinpoint here a key difference between the present case and the dynamics observed in the corresponding panels of the previous two figures. In particular, careful observation of panel (c) near $t = 200$ unravels an *oscillatory* evolution of both the central peak, as well as the two side peaks of the solution. This is something not obvious in the other real-valued configurations and stems from the fact that for the latter, the instability was principally triggered by a real eigenvalue pair (leading to pure exponential growth), while here the relevant mechanism involves a complex eigenvalue and hence favors an

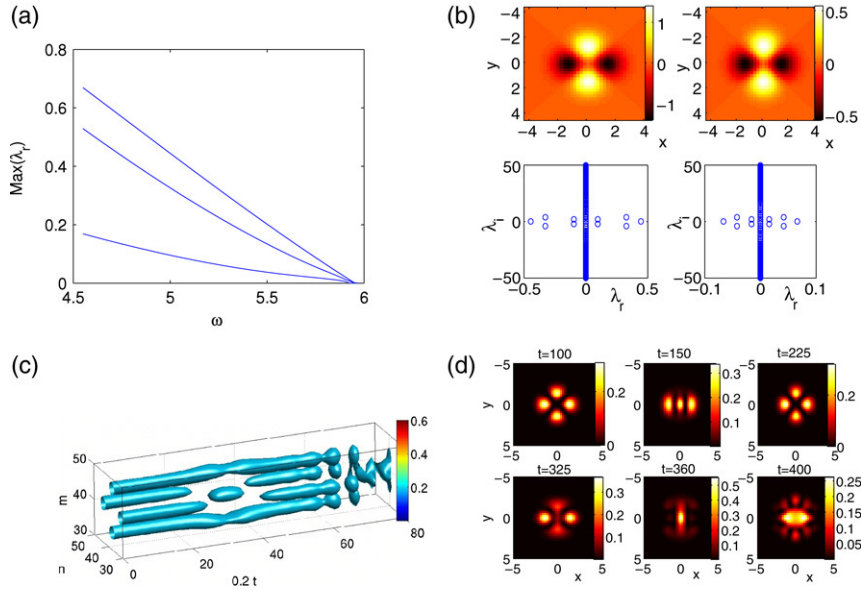


Fig. 4. (Color online) Similar as Fig. 3 but now for the multi-pole (quadrupole in this case with $\ell' = 2$) solution. Panel (a) shows the real parts of the most unstable eigenvalues, the largest one of which pertains to a real pair, while the others to quartets arising from Hamiltonian–Hopf bifurcations. One quartet bifurcates from $\lambda = i4$, while two quartets bifurcate from $\lambda = i2$. Panel (b) shows relevant details (configuration and its stability) for $\omega = 5$ (left) and $\omega = 5.8$ (right). Panel (c) shows the dynamical evolution of the configuration for $\omega = 5.8$ up to times $t = 400$, while panel (d) provides snapshots of the evolution at specific times.

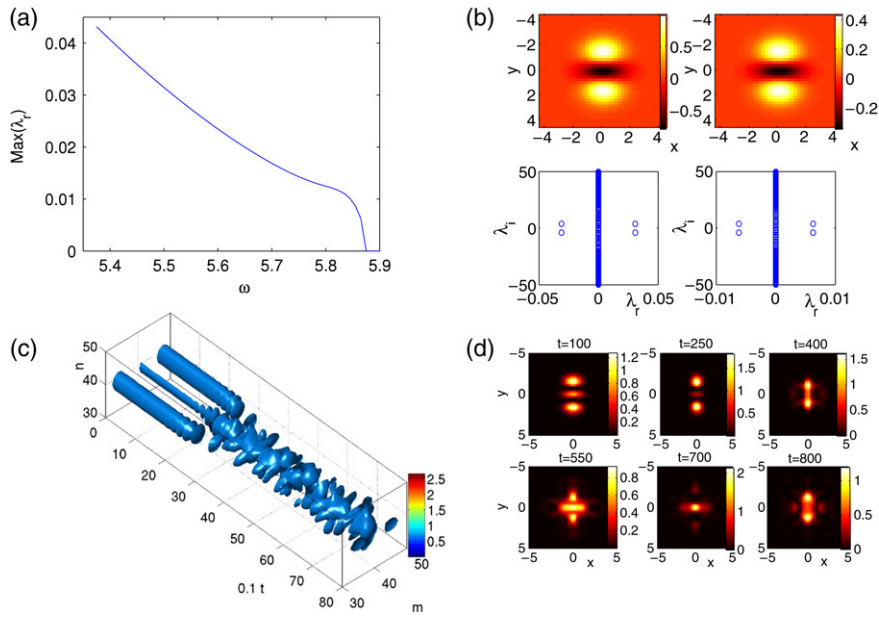


Fig. 5. (Color online) Same as the previous two solutions but now for the third real-valued solution, namely the soliton necklace. In this case the solution is unstable due to an eigenvalue quartet. Panels (b) show the solution for $\omega = 5.505$ and $\omega = 5.865$. Panel (c) shows its spatio-temporal evolution for $\omega = 5.375$, while panel (d) contains relevant snapshots of (c).

oscillatory instability development. The evolution at later times is rather complex and appears to involve alternations between more localized single-pulse configurations and less localized ones involving pulse pairs (or more complicated structures), as is shown in the snapshots of panel (d).

We now move to the complex-valued solutions, starting with the ring-like vortex solution of topological charge two in Fig. 6. In this case the solution becomes unstable due to a complex eigenvalue quartet, as shown in panels (a) and (b). This is in agreement with the theoretical findings of Lemma 6.7 (see also the relevant remark). In fact, zooming into the panel (b) of the figure illustrating both the spectral plane, as well as the solution (real and imaginary parts, amplitude, as well as phase), indicates that the pertinent bifurcation indeed emerges for our case of $\ell' = 2$ from $\lambda = \pm i4$. The instability of the solution is manifested through panels (c)

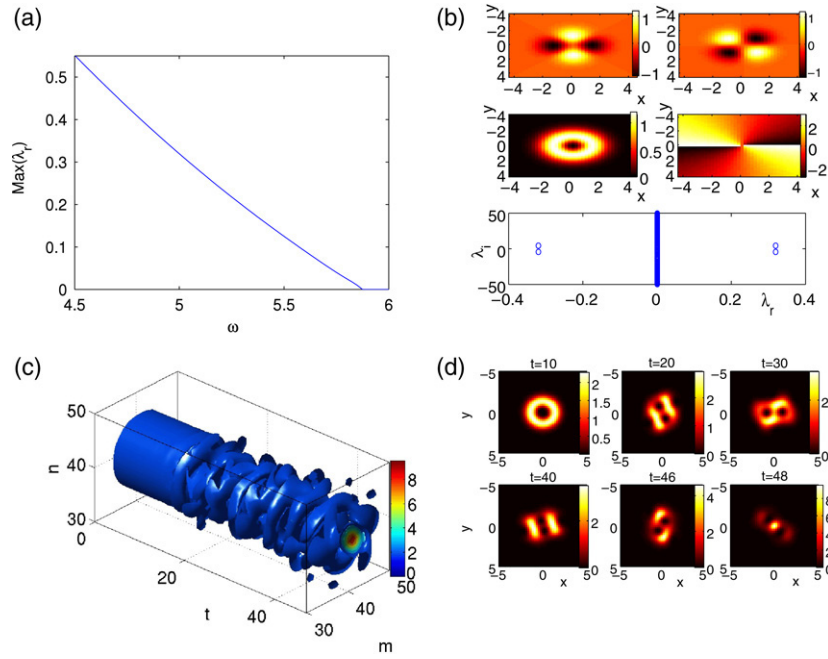


Fig. 6. (Color online) This figure is similar to the earlier ones but now for the vortex-like complex radial solution. Notice that now in panel (b) the configuration is only shown for $\omega = 5$, but the real and imaginary parts are shown in the top panel and the modulus and phase in the middle one. The bottom panel contains the relevant spectral plane, featuring again (see also panel (a)) a complex eigenvalue quartet. The evolution of panel (c) leads initially to a break-up into two single-charged vortices and eventually collapse as is shown in the snapshots of panel (d).

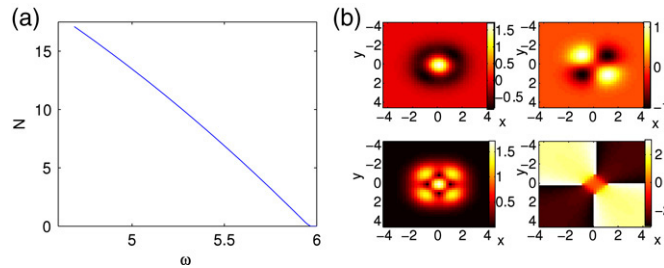


Fig. 7. (Color online) This figure shows the results for the stable vortex necklace branch complex solution. Panel (a) shows the squared L^2 norm of the branch (the number of particles N) as a function of the chemical potential; panel (b) shows the profile of the real (top left), imaginary (top right), modulus (bottom left) and phase (bottom right) of this solution for $\omega = 5$.

and (d) and illustrates the splitting of the doubly quantized vortex into two singly quantized ones due to the instability; see also the discussion of [50] and cf. with the repulsive case of [45], associated with the experimental results of [38,51]. In particular, we observe also split–merge cycles similarly to [50] as partially illustrated by the snapshots of panel (d), e.g., see the almost recombined vortices of $t = 40$ in comparison with the more separated ones at $t = 20, 30$ or $t = 46$. Eventually, the condensates collapse (shortly after the last subplot of panel (d) at $t = 48$).

Finally, we have also identified the sole generically stable branch of solutions (among the ones considered herein), by identifying the vortex necklace branch in the $\ell' = 2$ case, shown in Fig. 7. In this case, there is no eigenvalue with nonzero real part, and panel (a) shows the dependence of the squared L^2 norm (the number of particles) N on the chemical potential ω . The real and imaginary part (top), as well as the amplitude and phase (bottom) of a typical relevant solution, for $\omega = 5$ are shown in panel (b).

8. Two-ring solutions

Now that one-ring solutions have been thoroughly discussed, let us give a brief treatment of two-ring solutions. First, in order to apply the theory presented in the previous sections, one must first choose Ω so that the eigenvalue $\lambda_{2,0} = 10$ is semi-simple with multiplicity three. Setting $\lambda_{0,\ell'} = 10$ yields that

$$\Omega_{\ell'} = -2 + 8/\ell'. \tag{8.1}$$

Now, for $\Omega = \Omega_{\ell'}$ one has that

$$\lambda_{m,\ell} = 2 + 4m + 8\frac{\ell}{\ell'}$$

Setting $\lambda_{m,\ell} = 10$ yields the relationship

$$1 - \frac{1}{2}m = \frac{\ell}{\ell'} \tag{8.2}$$

Eq. (8.2) clearly holds for $(m, \ell) = (0, \ell')$ and $(m, \ell) = (2, 0)$. If $m = 1$, then Eq. (8.2) can be satisfied only if $\ell' = 2j$ for some $j \in \mathbb{N}$. Consequently, it will henceforth be assumed that $\ell' = 2j + 1$ for some $j \in \mathbb{N}$.

In order to continue, one must first compute the quantities as in Eq. (3.5). One sees that

$$\begin{aligned} g_0 &:= \int_0^\infty r q_{2,0}^4(r) dr = \frac{11}{128} \frac{1}{\pi^2} \\ g_{\ell'} &:= \int_0^\infty r q_{0,\ell'}^4(r) dr = \frac{(2\ell')!}{4^{\ell'} (\ell')^2} \frac{1}{\pi^2} \\ g_{0\ell'} &:= \int_0^\infty r q_{2,0}^2(r) q_{0,\ell'}^2(r) dr = \frac{\ell'^4 - 6\ell'^3 + 19\ell'^2 - 14\ell' + 24}{2^{\ell'+7}} \frac{1}{\pi^2}, \end{aligned} \tag{8.3}$$

and from these expressions one can immediately compute the quantities given in Eq. (3.6). Upon following the arguments presented in Section 3 one can eventually determine for which odd values of ℓ' a solution would exist. Examples of such solutions are given in Figs. 8 and 9.

In a similar manner, upon following the reasoning of Section 5 one can eventually generate the table regarding the location of the small eigenvalues given in Eq. (8.4). Since $k_c = 0$ in all cases, this quantity has not been included therein. Furthermore, if a field is blank, then this implies that a solution does not exist for that value of ℓ' . If $a = +1$, then in Eq. (8.4) one should interchange the entries associated with k_i^+ and k_i^- .

Solution	$a = -1$ (repulsive)											
	$\ell' = 3$			$\ell' = 5, 7$			$\ell' = 9$			$\ell' \geq 11$		
	k_r	k_i^-	k_i^+	k_r	k_i^-	k_i^+	k_r	k_i^-	k_i^+	k_r	k_i^-	k_i^+
<i>ring</i>	2	0	0	2	0	0	0	2	0	0	2	0
<i>multi-pole</i>	0	1	0	1	0	0	1	0	0	0	1	0
<i>soliton necklace</i>				0	1	0				1	0	0
<i>vortex</i>	0	1	1	0	0	2	0	0	2	0	1	1
<i>vortex necklace</i>	0	1	0	0	1	0	0	1	0	0	1	0

The Hamiltonian–Hopf bifurcation calculations will proceed in a manner similar to that presented in Section 6. The primary difference is that Eq. (6.11) now becomes

$$\begin{aligned} (a, b) = (0, 0): (c, d) &\in \{(0, 2\ell'), (2, \ell'), (4, 0)\} \\ (a, b) = (0, \ell): (c, d) &\in \{(0, 2\ell' - \ell), (2, \ell' - \ell)\}, \quad \ell = 1, \dots, \ell' - 1 \\ (a, b) = (1, 0): (c, d) &\in \{(1, \ell'), (3, 0)\} \\ (a, b) = (1, \ell): (c, d) &\in \{(1, \ell' - \ell)\}, \quad \ell = 1, \dots, \frac{1}{2}(\ell' - 1). \end{aligned} \tag{8.5}$$

Those eigenvalues associated with $a = 0$ are semi-simple with multiplicity six and associated with the eigenvalues $\lambda = \pm i8\ell/\ell'$ ($\ell = 1, \dots, \ell'$), while those with $a = 1$ are semi-simple with multiplicity four and associated with the eigenvalues $\lambda = \pm i4(2\ell + 1)/\ell'$ ($\ell = 0, \dots, [\ell' - 1]/2$). Thus, at this level the primary difference between the one-ring and two-ring structures is the possibility of having additional mode interactions which may lead to more Hamiltonian–Hopf bifurcations.

When considering the vortex solution, it turns out to be the case that the calculations presented in Section 6.3.1 yield a complete picture for $\lambda = \pm i4(1 + \ell/\ell')$, $\ell = 1, \dots, \ell'$. For $\lambda = \pm i4\ell/\ell'$, $\ell = 1, \dots, \ell'$, however, more complicated mode interactions than those discussed in Section 6.3.1 are possible, i.e., for these values of λ it is possible to have interactions between the $a = 0$ modes and that $a = 1$ modes. The final result is that the vortex will be at least as unstable in the two-ring case as in the one-ring case. The calculations and results associated with all of the other solutions will be left for the interested reader.

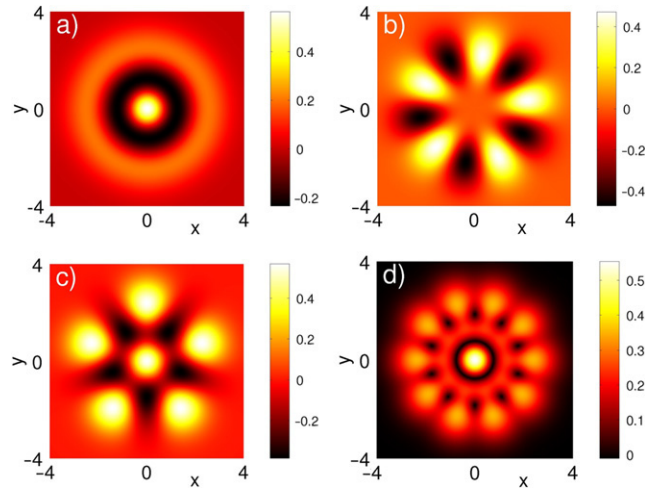


Fig. 8. (Color online) Some of the solutions to Eq. (3.1) when $\ell' = 5$, and for $\Omega = \Omega_{\ell'} (= -2/5)$ given in Eq. (8.1). Panels (a)–(c) correspond to real-valued solutions, whereas panel (d) depicts the modulus of a complex-valued solution. These solutions correspond to: (a) ring, (b) multi-pole, (c) soliton necklace, and (d) vortex necklace.

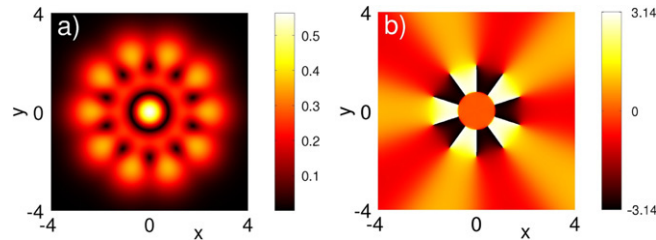


Fig. 9. (Color online) The vortex necklace solution to Eq. (3.1) when $\ell' = 5$ (see panel (d) in Fig. 8). Panel (a) depicts the modulus of the solution, and panel (b) its phase.

9. Conclusions and future challenges

In the present paper we have offered a systematic analysis of the wealth of solutions of the nonlinear problem of rotating Bose–Einstein condensates in the presence of parabolic trapping potentials. We have illustrated the usefulness of examining the underlying linear limit of the problem and the relevance of using the Lyapunov–Schmidt method to establish the existence of the solutions. The approach of examining a perturbative reduction of the original problem has also been successfully applied to the linearization around the obtained waveforms. This has yielded information both about the small eigenvalues near the origin of the spectral plane, as well as about $\mathcal{O}(1)$ eigenvalues potentially subject to Hamiltonian–Hopf bifurcations.

We have exemplified the approach through identifying five different classes of solutions, three of which are real-valued and two of which are complex-valued. Among them, one can identify previously analyzed theoretically [31,45,49,50] and even produced experimentally [38,51] vortex solutions of topological charge higher than one. We have also examined previously reported ring soliton solutions [53] (see also [12] for a recent discussion), recently identified multi-pole solutions [40], as well as necklace structures consisting of solitons or vortices. For all of these coherent structures the stability has been identified, revealing that only vortex necklaces are typically stable among these complex structures. The analytical results have been corroborated by numerical simulations confirming the sources of instability of the various solutions and also showcasing the manifestation of these instabilities in direct numerical experiments.

It should be noted here that while some of the simpler pertinent structures have already been experimentally produced in BECs, recent optical advances in producing amplitude and phase masks have made it possible to imprint on liquid crystal displays structures such as the ones discussed here. In particular, the recent work of [9] renders possible, through the use of helical Ince–Gaussian beams, the generation of single- and multi-ring structures, including soliton and vortex necklaces (see [9, Figs. 1–3] for details). Application of such input conditions to BECs could provide a convenient method for the generation of some of the more complex structures analyzed herein. Finally, on the theoretical side it is natural to inquire how the waveforms obtained herein generalize in three-dimensional settings (e.g., see [15]). Another straightforward question concerns the outcome of appending additional rings of structures, such as vortex rings, in the solution in an attempt to semi-analytically construct vortex lattice solutions. Such directions are currently being investigated and will be reported in future publications.

Acknowledgments

PGK gratefully acknowledges the support of NSF-DMS-0204585 and NSF-CAREER, and numerous discussions with D.J. Frantzeskakis in the initial stages of this work. PGK and RCG also acknowledge the support of NSF-DMS-0505663. The work of TK is partially supported by the NSF under grant DMS-0304982, and by the ARO under grant 45428-PH-HSI.

References

- [1] N. Abdallah, F. Méhats, C. Schmeiser, R. Weishäupl, The nonlinear Schrödinger equation with a strongly anisotropic harmonic potential, *SIAM J. Math. Anal.* 37 (1) (2005) 189–199.
- [2] F. Abdullaev, R. Kraenkel, Coherent atomic oscillations and resonances between coupled Bose–Einstein condensates with time-dependent trapping potential, *Phys. Rev. A* 62 (2000) 023613.
- [3] J.R. Abo-Shaer, C. Raman, J.M. Vogels, W. Ketterle, Observation of vortex lattices in Bose–Einstein condensates, *Science* 292 (5516) (2001) 476–479.
- [4] G. Agrawal, *Nonlinear Fiber Optics*, third edition, Academic Press, 2001.
- [5] B. Anderson, K. Dholakia, E. Wright, Atomic-phase interference devices based on ring-shaped Bose–Einstein condensates: Two-ring case, *Phys. Rev. A* 67 (3) (2003) 033601.
- [6] K. Atkinson, *An Introduction to Numerical Analysis*, second edition, John Wiley and Sons, 1989.
- [7] Y.B. Band, I. Towers, B.A. Malomed, Unified semiclassical approximation for Bose–Einstein condensates: Application to a BEC in an optical potential, *Phys. Rev. A* 67 (2003) 023602.
- [8] R. Battyé, N. Cooper, P. Sutcliffe, Stable Skyrmions in two-component Bose–Einstein condensates, *Phys. Rev. Lett.* 88 (8) (2002) 080401.
- [9] J.B. Bentley, J.A. Davis, M.A. Bandres, J.C. Gutiérrez-Vega, Generation of helical Ince–Gaussian beams with liquid-crystal display, *Opt. Lett.* 31 (5) (2006) 649–651.
- [10] R. Bradley, B. Deconinck, J. Kutz, Exact nonstationary solutions to the mean-field equations of motion for two-component Bose–Einstein condensates in periodic potentials, *J. Phys. A* 38 (2005) 1901–1916.
- [11] T. Busch, J. Cirac, V. Pérez-García, P. Zoller, Stability and collective excitations of a two-moment Bose–Einstein condensed gas: A moment approach, *Phys. Rev. A* 56 (4) (1997) 2978–2983.
- [12] L.D. Carr, C.W. Clark, Vortices and ring solitons in Bose–Einstein condensates, *Phys. Rev. A* 74 (2006) 043613.
- [13] P. Chossat, R. Lauterbach, *Methods in Equivariant Bifurcations and Dynamical Systems*, in: *Advanced Series in Nonlinear Dynamics*, vol. 15, World Scientific, 2000.
- [14] L.-C. Crasovan, G. Monina-Terriza, J. Torres, L. Torner, V. Pérez-García, D. Mihalache, Globally linked vortex clusters in trapped wave fields, *Phys. Rev. E* 66 (3) (2002) 036612.
- [15] L.-C. Crasovan, V. Pérez-García, I. Danaila, D. Mihalache, L. Torner, Three-dimensional parallel vortex rings in Bose–Einstein condensates, *Phys. Rev. A* 70 (3) (2004) 033605.
- [16] F. Dalfovo, S. Giorgini, L. Pitaevskii, S. Stringari, Theory of Bose–Einstein condensation in trapped gases, *Rev. Modern Phys.* 71 (1999) 463–512.
- [17] J.A. Davis, J.B. Bentley, Azimuthal prism effect with partially blocked vortex-producing lenses, *Opt. Lett.* 30 (2005) 3204–3206.
- [18] V.V. Kotlyar, A.A. Kovalev, V.A. Soifer, C.S. Tuvey, J.A. Davis, Sidelobe contrast reduction for optical vortex beams using helical axicon, *Opt. Lett.* 32 (2007) 921–923.
- [19] P. Engels, I. Coddington, P.C. Haljan, E.A. Cornell, Nonequilibrium effects of anisotropic compression applied to vortex lattices in Bose–Einstein condensates, *Phys. Rev. Lett.* 89 (10) (2002) 100403.
- [20] N. Ginsberg, J. Brand, L. Hau, Observation of hybrid soliton vortex-ring structures in Bose–Einstein condensates, *Phys. Rev. Lett.* 94 (4) (2005) 040403.
- [21] M. Grillakis, Linearized instability for nonlinear Schrödinger and Klein–Gordon equations, *Comm. Pure Appl. Math.* 46 (1988) 747–774.
- [22] Y.J. He, H.H. Fan, J.W. Dong, H.Z. Wang, Self-trapped spatiotemporal necklace–ring solitons in the Ginzburg–Landau equation, *Phys. Rev. E* 74 (2006) 016611.
- [23] M. Hărăguș, T. Kapitula, On the spectra of periodic waves for infinite-dimensional Hamiltonian systems. <http://www.math.unm.edu/~kapitula/papers/PeriodicWaveSubmission.pdf>, 2007.
- [24] J.k. Kim, A. Fetter, Dynamics of a single ring of vortices in two-dimensional trapped Bose–Einstein condensates, *Phys. Rev. A* 70 (4) (2004) 043624.
- [25] T. Kapitula, P. Kevrekidis, Bose–Einstein condensates in the presence of a magnetic trap and optical lattice, *Chaos* 15 (3) (2005) 037114.
- [26] T. Kapitula, P. Kevrekidis, B. Sandstede, Counting eigenvalues via the Krein signature in infinite-dimensional Hamiltonian systems, *Physica D* 195 (3–4) (2004) 263–282.
- [27] T. Kapitula, P. Kevrekidis, B. Sandstede, Addendum: Counting eigenvalues via the Krein signature in infinite-dimensional Hamiltonian systems, *Physica D* 201 (1–2) (2005) 199–201.
- [28] T. Kapitula, P. Kevrekidis, Z. Chen, Three is a crowd: Solitary waves in photorefractive media with three potential wells, *SIAM J. Appl. Dyn. Syst.* 5 (4) (2006) 598–633.
- [29] K. Kasamatsu, M. Tsubota, M. Ueda, Quadrupole and scissors modes and nonlinear mode coupling in trapped two-component Bose–Einstein condensates, *Phys. Rev. A* 69 (4) (2004) 043621.
- [30] T. Kato, *Perturbation Theory for Linear Operators*, Springer-Verlag, Berlin, 1980.
- [31] Y. Kawaguchi, T. Ohmi, Splitting instability of a multiply charged vortex in a Bose–Einstein condensate, *Phys. Rev. A* 70 (4) (2004) 043610.
- [32] P. Kevrekidis, D. Frantzeskakis, Pattern forming dynamical instabilities of Bose–Einstein condensates, *Modern Phys. Lett. B* 18 (2004) 173–202.
- [33] P. Kevrekidis, H. Nistazakis, D. Frantzeskakis, B. Malomed, R. Carretero-González, Families of matter-waves in two-component Bose–Einstein condensates, *Eur. Phys. J. D* 28 (2004) 181–185.
- [34] P.G. Kevrekidis, R. Carretero-González, D.J. Frantzeskakis, I.G. Kevrekidis, Vortices in Bose–Einstein condensates: Some recent developments, *Modern Phys. Lett. B* 18 (30) (2004) 1481–1505.
- [35] Yu.S. Kivshar, G. Agrawal, *Optical Solitons: From Fibers to Photonic Crystals*, Academic Press, 2003.
- [36] R. Kollár, R. Pego, Stability of vortices in two-dimensional Bose–Einstein condensates: A mathematical approach. Preprint.
- [37] V.V. Konotop, V.A. Brazhnyi, Dynamics of Bose–Einstein condensates in optical lattices, *Modern Phys. Lett. B* 18 (14) (2006) 179–215.
- [38] A.E. Leanhardt, A. Görlitz, A.P. Chikkatur, D. Kielpinski, Y. Shin, D.E. Pritchard, W. Ketterle, Imprinting vortices in a Bose–Einstein condensate using topological phases, *Phys. Rev. Lett.* 89 (19) (2002) 190403.

- [39] A. Leggett, Bose–Einstein condensation in the alkali gases: Some fundamental concepts, *Rev. Modern Phys.* 73 (2001) 307–356.
- [40] M. Liu, L. Wen, H. Xiong, M. Zhan, Structure and generation of the vortex–antivortex superposed state in Bose–Einstein condensates, *Phys. Rev. A* 73 (6) (2006) 063620.
- [41] R. MacKay, Stability of equilibria of Hamiltonian systems, in: R. MacKay, J. Meiss (Eds.), *Hamiltonian Dynamical Systems*, Adam Hilger, 1987, pp. 137–153.
- [42] K.W. Madison, F. Chevy, W. Wohlleben, J. Dalibard, Vortex formation in a stirred Bose–Einstein condensate, *Phys. Rev. Lett.* 84 (2000) 806–809.
- [43] M. Matthews, B. Anderson, P. Haljan, D. Hall, C. Wieman, E. Cornell, Vortices in a Bose–Einstein condensate, *Phys. Rev. Lett.* 83 (13) (1999) 2498–2501.
- [44] O. Morsch, M. Oberthaler, Theory of nonlinear matter waves in optical lattices, *Rev. Modern Phys.* 78 (2006) 179–215.
- [45] M. Möttönen, T. Mizushima, T. Isoshima, M.M. Salomaa, K. Machida, Splitting of a doubly quantized vortex through intertwining in Bose–Einstein condensates, *Phys. Rev. A* 68 (2003) 023611.
- [46] D. Pelinovsky, J. Yang, Instabilities of multihump vector solitons in coupled nonlinear Schrödinger equations, *Stud. Appl. Math.* 115 (1) (2005) 109–137.
- [47] C.J. Pethick, H. Smith, *Bose–Einstein condensation in Dilute Gases*, Cambridge University Press, 2002.
- [48] L.P. Pitaevskii, S. Stringari, *Bose–Einstein Condensation*, Oxford University Press, 2003.
- [49] H. Pu, C. Law, J. Eberly, N. Bigelow, Coherent disintegration and stability of vortices in trapped Bose condensates, *Phys. Rev. A* 59 (2) (1999) 1533–1537.
- [50] H. Saito, M. Ueda, Split–merge cycle, fragmented collapse, and vortex disintegration in rotating Bose–Einstein condensates with attractive interactions, *Phys. Rev. A* 69 (1) (2004) 013604.
- [51] Y. Shin, M. Saba, M. Vengalattore, T.A. Pasquini, C. Sanner, A.E. Leanhardt, M. Prentiss, D.E. Pritchard, W. Ketterle, Dynamical instability of a doubly quantized vortex in a Bose–Einstein condensate, *Phys. Rev. Lett.* 93 (16) (2004) 160406.
- [52] K. Staliunas, S. Longhi, G.J. de Valcárcel, Faraday patterns in Bose–Einstein condensates, *Phys. Rev. Lett.* 89 (21) (2002) 210406.
- [53] G. Theocharis, D. Frantzeskakis, P.G. Kevrekidis, B. Malomed, Yu.S. Kivshar, Ring dark solitons and vortex necklaces in Bose–Einstein condensates, *Phys. Rev. Lett.* 90 (2003) 120403.